



## The *Zymoseptoria tritici* white collar-1 gene, *ZtWco-1*, is required for development and virulence on wheat

Anna M.M Tiley<sup>a,b,\*</sup>, Colleen Lawless<sup>b,c</sup>, Paola Pilo<sup>b</sup>, Sujit J. Karki<sup>b</sup>, Jijun Lu<sup>b</sup>, Zhuowei Long<sup>b</sup>, Hesham Gibriel<sup>b,d</sup>, Andy M. Bailey<sup>e</sup>, Angela Feechan<sup>b,\*</sup>

<sup>a</sup> Agri-Food Biosciences Institute, 18a Newforge Ln, Belfast BT9 5PX, United Kingdom

<sup>b</sup> School of Agriculture and Food Science, University College Dublin, Dublin 4, Republic of Ireland

<sup>c</sup> School of Biology and Environmental Science, University College Dublin, Dublin 4, Republic of Ireland

<sup>d</sup> Royal College of Surgeons in Ireland, Dublin 2, Ireland

<sup>e</sup> School of Biological Sciences, University of Bristol, 24 Tyndall Avenue, Bristol BS8 1TQ, United Kingdom

### ARTICLE INFO

#### Keywords:

*Zymoseptoria tritici*  
Wheat  
Light  
White collar

### ABSTRACT

The fungus *Zymoseptoria tritici* causes Septoria Tritici Blotch (STB), which is one of the most devastating diseases of wheat in Europe. There are currently no fully durable methods of control against *Z. tritici*, so novel strategies are urgently required. One of the ways in which fungi are able to respond to their surrounding environment is through the use of photoreceptor proteins which detect light signals. Although previous evidence suggests that *Z. tritici* can detect light, no photoreceptor genes have been characterised in this pathogen. This study characterises *ZtWco-1*, a predicted photoreceptor gene in *Z. tritici*. The *ZtWco-1* gene is a putative homolog to the blue light photoreceptor from *Neurospora crassa*, *wc-1*. *Z. tritici* mutants with deletions in *ZtWco-1* have defects in hyphal branching, melanisation and virulence on wheat. In addition, we identify the putative circadian clock gene *ZtFrq* in *Z. tritici*. This study provides evidence for the genetic regulation of light detection in *Z. tritici* and it opens avenues for future research into whether this pathogen has a circadian clock.

### 1. Introduction

Light is a key environmental signal that can be used by living organisms to detect and evaluate their surrounding environment. Fungi detect and react to light, and this signal can be used to regulate key biological processes such as developmental transition, secondary metabolism, virulence and sporulation (reviewed in Corrochano, 2019; Fuller et al., 2015; Idnurm et al., 2010; Rodríguez-Romero et al., 2010).

Fungi respond to light through the use of specialised photoreceptor proteins that sense blue, red, and green light (reviewed in Yu and Fischer, 2019). Photoreceptors are associated with light-absorbing molecules termed chromophores that absorb light, causing a conformational change in the photoreceptor protein structure. This conformational change affects the protein activity, and the photoreceptor can either directly control downstream gene expression or influence transcriptional machinery via other signalling modules (reviewed in Corrochano, 2019; Fischer et al., 2016; Schumacher, 2017; Yu and Fischer, 2019).

The first cloned fungal photoreceptor gene was *white collar-1* (*wc-1*) from *Neurospora crassa*, and this was followed shortly by the cloning of *white collar-2* (*wc-2*) (Ballario et al., 1996; Linden and Macino, 1997). Both the WC-1 and WC-2 proteins contain a PER-ARNT-SIM (PAS) domain for protein interaction and a zinc-finger DNA-binding domain (Ballario et al., 1998, 1996; Talora et al., 1999). The WC-1 protein also contains a Light-, Oxygen-, and Voltage-sensing (LOV) domain which binds to a flavin (FAD) chromophore (Ballario et al., 1998; Froehlich et al., 2002; He et al., 2002). WC-1 and WC-2 interact to form the heterodimeric White Collar Complex (WCC) which has a role both as a blue light photosensor and transcription factor in *N. crassa* (Talora et al., 1999). In addition to its role in the *N. crassa* light response, the WCC coordinates the *N. crassa* circadian clock through interaction with the *frequency* gene product (FRQ) (reviewed in Baker et al., 2012; Dunlap and Loros, 2006).

Since the identification of the WCC in *N. crassa*, White Collar protein homologs have been identified in species of fungal lineages including the Ascomycota e.g. *Aspergillus nidulans* (Purschwitz et al., 2008),

\* Corresponding authors at: Agri-Food Biosciences Institute, 18a Newforge Ln, Belfast BT9 5PX, United Kingdom (A.M.M. Tiley). School of Agriculture and Food Science, University College Dublin, Dublin 4, Republic of Ireland (A. Feechan).

E-mail addresses: [anna.tiley@afbini.gov.uk](mailto:anna.tiley@afbini.gov.uk) (A.M.M Tiley), [angela.feechan@ucd.ie](mailto:angela.feechan@ucd.ie) (A. Feechan).

<https://doi.org/10.1016/j.fgb.2022.103715>

Received 14 October 2021; Received in revised form 2 June 2022; Accepted 6 June 2022

Available online 14 June 2022

1087-1845/Crown Copyright © 2022 Published by Elsevier Inc. This is an open access article under the CC BY license (<http://creativecommons.org/licenses/by/4.0/>).

Basidiomycota e.g. *Cryptococcus neoformans* (Idnurm and Heitman, 2005) and Mucoromycota e.g. *Phycomyces blakesleeanus* (Idnurm et al., 2006). As a result, the White Collar proteins are considered to be the most conserved photoreceptors in the fungal kingdom.

More recently, the role of White Collar proteins in virulence of plant pathogenic fungi have been investigated. For example, White Collar gene homologs have a role in sporulation in the wheat pathogen *Fusarium graminearum* and in the maize pathogen *Ustilago maydis* (H. Kim et al., 2015; Sánchez-Arreguin et al., 2020). In addition to their roles in sporulation and development, White Collar proteins have been demonstrated to be involved in virulence. Disruption of the *Cercospora* regulator of pathogenesis gene (*CRP1*) in the maize pathogen *Cercospora zea-maydis* impacts hyphal tropism towards the stomata, appressoria formation and biosynthesis of cercosporin (H. Kim et al., 2011). To date, the best studied example of the light response and the White Collar homolog in a plant pathogenic fungus is in *Botrytis cinerea* (Schumacher, 2017). Research on the *B. cinerea* *wc-1* and *wc-2* genes (*bcwcl1* and *bcwcl2*) demonstrated that these genes have roles in differentiation, oxidative stress tolerance and virulence (Canessa et al., 2013). In addition, the BCWCL1 protein is involved in regulating the *B. cinerea* circadian clock through interaction with the *B. cinerea* FREQUENCY homolog (BCFRQ) (Hevia et al., 2015).

*Zymoseptoria tritici* is a major pathogen of wheat, and the greatest threat to wheat production in countries such as the UK and Ireland (Fones and Gurr, 2015; Torriani et al., 2015). This ascomycete pathogen infects wheat by entering the leaf exclusively through the stomata (Duncan and Howard, 2000; Kema et al., 1996). Infection is characterised by a long symptomless period which lasts approximately 9–17 days, during which the pathogen grows extracellularly within the leaf (Duncan and Howard, 2000; Kema et al., 1996; Keon et al., 2007). This is followed by the necrotrophic period of infection which is characterised by chlorosis and necrosis of the leaf tissue (Keon et al., 2007; Shetty et al., 2007). Asexual and sexual fruiting bodies (pycnidia and pseudothecia respectively) are produced in the necrotic lesions on the leaf and these release the asexual pycnidiospores and sexual ascospores (Eyal et al., 1987).

Previous studies have demonstrated that infection of wheat by *Z. tritici* is promoted by light (Benedict, 1971). In addition, darkness can have a negative impact on infection by *Z. tritici* and it can delay symptom development (Fellows, 1962; Keon et al., 2007). However, the influence of light varies depending on whether illumination occurs early or later in infection (Shaw, 1991). Therefore, it is possible that the time of day may influence outcome of *Z. tritici* infection in the field. Previous findings are from *in planta* experiments and it is therefore difficult to separate the pathogen's response to light from those caused indirectly due to the host plant's response to light. Therefore, *in vitro* studies and mutant analyses can help to elucidate the role of light in *Z. tritici* development and infection.

In addition to a role in infection, light has also been shown to affect *Z. tritici* development. For example, light intensities of 16, 000 and 20, 000 lx promote hyphal elongation and formation of conidia on wheat extract agar (Benedict, 1971). In addition, *Z. tritici* cultures melanise faster under constant dark conditions compared to 12:12 light:dark cycles (Tiley et al., 2019). *Z. tritici* can also respond to different light wavelengths and it produces more aerial hyphae under constant blue light regimes compared to constant red light (Choi and Goodwin, 2011). Recent transcriptomic analyses comparing *Z. tritici* cultures incubated under white, blue or red light and complete darkness demonstrate that this pathogen is capable of sensing and responding to different light wavelengths (McCorison and Goodwin, 2020).

Despite mounting evidence that *Z. tritici* can detect and respond to light, no photoreceptor genes have been characterised in this species until now. In this study we characterise the first putative photoreceptor gene in *Z. tritici*, *white collar-1* (*ZtWco-1*). We demonstrate that *ZtWco-1* is essential for melanisation, hyphal branching and virulence in *Z. tritici*. In addition, we identify the putative homolog to the *N. crassa* frequency

gene (*frq*) in *Z. tritici*. Findings from this research open multiple avenues for further study into the role of light and periodicity during *Z. tritici* infection of wheat, and the identification of novel control strategies against this economically important pathogen of wheat.

## 2. Materials and methods

### 2.1. Fungal strains and media

The *Zymoseptoria tritici* IPO323 strain was used throughout this study (obtained from Prof. G. Kema) (Kema and van Silfhout, 1997). Fungal strains were incubated at 20 °C and cultured on either PDA (24 g/L potato dextrose broth and 20 g/L technical agar), Czapek Dox-V8 juice (CDV8) agar (46 g/L Czapek Dox agar, 200 ml/L V8® Original Vegetable juice (Campbell Soup Company), 3 g/L calcium carbonate and 20 g/L technical agar) or YPDA agar (10 g/L yeast extract, 20 g/L peptone, 20 g/L glucose and 20 g/L technical agar). All Petri dishes were sealed with double layers of Parafilm® M to exclude the impact of gas exchange on experimental setup. Solid media cultures were incubated under either 12:12 light:dark (LD) cycles, constant light (LL), or the Petri dishes were wrapped in double layers of foil for constant dark conditions (DD). Lighting conditions were white light (WL) (Phillips bulbs TLD 36–33 W, at approximately 2300 lx) or white light supplemented with UV-A (WL-UVA) (Phillips bulbs TLD 36–33 W – TL-D 36 W BLB (Hg), at approximately 1400 lx) to induce asexual sporulation. Growth comparison on solid media was carried out by inoculating the Petri dish with a 10 µl drop from a serial dilution of  $1 \times 10^6$  –  $1 \times 10^4$  spores/ml. Three to four Petri dishes were inoculated per strain and per condition, and experiments were repeated three times independently. Liquid media experiments used liquid potato dextrose broth (PDB 24 g/L) inoculated with a final concentration of  $1 \times 10^4$  spores/ml and incubated at 200 rpm and 20 °C for 7 days post-inoculation (dpi). Two to three flasks were inoculated per strain and experiments were repeated twice independently.

### 2.2. In vitro light detection experiment

Light detection experiments were carried out using wheat extract agar (37.5 g/L homogenised fresh wheat leaves cv. Dunmore, 20 g/L technical Agar) as outlined in Tiley et al. (2018). Petri dishes were inoculated with yeast-like cells from *Z. tritici* IPO323 cultures previously grown on CDV8 agar under LL WL conditions at 20 °C. Following inoculation, Petri dishes were sealed with double layers of Parafilm® M and incubated under LL, WL or DD conditions at 20 °C for 58 days. The experiment was repeated independently three times with four Petri dishes tested under each light condition per independent experiment.

### 2.3. Detached leaf assays

A modified version of the detached leaf assay protocol outlined by (Arraiano et al., 2001; Chartrain et al., 2004) was used. Wheat cv. Riband was grown under 16:8 LD cycles in WL at 20 °C until growth stage 12–13 (Tottman, 1987). An 8 cm section of the first true leaf of each wheat plant was used for the experiment. *Z. tritici* cells were grown on CDV8 for 3–5 days under DD conditions at 20 °C. The *Z. tritici* cells were suspended to  $1 \times 10^6$  spores/ml in 0.01 % Tween 20. The spore suspension was sprayed onto the wheat leaves fifteen times using a hand-held sprayer. Leaves sprayed with 0.01 % Tween 20 were used as the negative control.

Double-strength water agar (40 g/L) containing Benzimidazole (100 mg/L) was dispensed into square Petri dishes and the agar was cut into four strips of equal size. The wheat leaves were secured at the tip and base between two strips of agar, adaxial-side-up. Each Petri dish contained between 5 and 7 wheat leaves. Petri dishes containing the infected leaves or the negative control leaves were sealed with double layers of Parafilm® M and incubated under LL (WL – UVA) to induce

asexual sporulation or DD for 21 days. The experiment was repeated independently twice and between three to four Petri dishes were tested per condition.

#### 2.4. Identification of *ZtWco-1*, *ZtWco-2* and *ZtFrq*

The published genome of *Z. tritici* IPO323 was used throughout this study to identify and characterise potential *ZtWco-1*, *ZtWco-2* and *ZtFrq* gene homologs in this pathogen (Goodwin et al., 2011). The known WC-1, WC-2 and FRQ FASTA protein sequences from the model ascomycete fungi including *Neurospora crassa*, *Aspergillus nidulans*, *Botrytis cinerea*, *Trichoderma reesei*, *Magnaporthe oryzae* and *Fusarium graminearum* were queried against the *Z. tritici* genome database (<https://genome.jgi-psf.org/Mycgr3/Mycgr3.home.html>, last accessed May 2022) using the tblastn and Filtered Models (transcripts) algorithms. More than one BLAST match occurred in *Z. tritici* for the WC-1 and WC-2 FASTA sequences. Best Bidirectional Blast Hit was carried out using the National Centre for Biotechnology Information (NCBI) database (<https://blast.ncbi.nlm.nih.gov/>, last accessed May 2022) protein–protein blast (blastp) against the nonredundant protein sequences database of each model ascomycete. The putative homologs to WC-1 and WC-2 in *Z. tritici* were aligned with the sequences from other fungi using Clustal W in RStudio using the “MSA” package (Larkin et al., 2007; Bodenhofer et al., 2015; Rstudio Team, 2020). IQ-Tree was used to create maximum likelihood phylogenetic trees with a bootstrap test at 1000 replicates, and model finder was used to determine the best substitution model (Nguyen et al., 2015; Trifinopoulos et al., 2016; Kalyaanamoorthy et al., 2017). The best fitting model for the WCO-1 and WCO-2 trees were JTT + F + I + G4 and LG + F + I + G4 respectively. Phylogenetic trees were visualised using iTOL with rooting on the Mucoromycota outgroup (Letunic and Bork, 2006; Letunic and Bork, 2021).

The IPO323 annotation of the *ZtWco-1*, *ZtWco-2* and *ZtFrq* genes were manually inspected using the Web Apollo editing platform (Lee et al., 2013). The intron/exon boundaries and/or missing untranslated regions of *ZtWco-2* were reannotated to correct the gene structure using *Z. tritici* RNA-seq reads from 9 dpi (Rudd et al., 2015) mapped to the *Z. tritici* IPO323 reference genome (Goodwin et al., 2011).

Visual inspection of the *Z. tritici* ZTWCO-1 (Mycgr3\_76651), ZTWCO-2 (Mycgr3\_32587) and ZTFRQ (Mycgr3\_93972) FASTA sequences was carried out using InterProScan (<https://www.ebi.ac.uk/interpro/>, last accessed May 2022) (Blum et al., 2021). This was used to infer the presence of predicted PAS domains, GATA-type zinc finger domain and conserved regions typically associated with LOV domains.

#### 2.5. Protein 3D structure and function Prediction methods

3D structural template models for ZTWCO-1 and ZTWCO-2 were predicted using the I-TASSER (Iterative Threading ASSEMBLY Refinement) server (<https://zhanglab.ccmb.med.umich.edu/I-TASSER>, last accessed March 2022). The I-TASSER server builds the 3D models for ZTWCO-1 and ZTWCO-2 by reassembling fragments excised from threading templates (Yang and Zhang, 2015; Zhang et al., 2017). The confidence score produced by I-TASSER is usually within the range of –5 and 2 and is used to estimate the quality of the predicted models. A score of higher value indicates a model with a high confidence (Yang and Zhang, 2015; Zhang et al., 2017). The highest c-scoring model for ZTWCO-1 and ZTWCO-2 was subsequently used for visualising protein–protein interactions (Katebi et al., 2010). The ClusPro server (<https://cluspro.org>) was used for protein–protein docking in 3D format (Desta et al., 2020; Kozakov et al., 2017, 2013; Vajda et al., 2017). UCSF Chimera (developed from the Resource for Biocomputing, Visualization, and Informatics at the University of California, San Francisco with support from NIH P41 RR-01081 and available from <https://www.cgl.ucsf.edu/chimera/>, last accessed May 2022) was used for visualising the molecular graphics of the 3D modelled proteins and molecular protein docking (Petersen et al., 2004). Predicted Gene Ontology (GO) for both

proteins were carried out using the online server (<https://zhanggroup.org/MetaGO/>, last accessed March 2022) to identify predicted molecular function terms for ZTWCO-1 and ZTWCO-2 (Zhang et al., 2018). The MetaGO server produces a confidence score for predicted GO terms. Confidence values range in between 0 and 1; where a higher value indicates a better confidence (Zhang et al., 2018).

#### 2.6. Yeast two-hybrid analysis

The interaction of *Z. tritici* ZTWCO-1 and ZTWCO-2 was tested using yeast two-hybrid (Y2H) analysis. The coding sequences of *ZtWco-1* and *ZtWco-2* were obtained from the *Z. tritici* genome database (<https://genome.jgi-psf.org/Mycgr3/Mycgr3.home.html>, last accessed May 2022) and amplified by PCR using gene specific primers (Supporting Table 1). PCR conditions were as follows: 1 cycle of 2 mins at 95 °C; 1 cycle of 30 s at 95 °C, 35 cycles of 30 s at 58 °C, 1 cycle at 72 °C for 3.5 min (*ZtWco-1*) OR 2 min (*ZtWco-2*) and a final cycle of 5 min at 72 °C followed by 4 °C holding temperature. *ZtWco-1* and *ZtWco-2* were cloned into the vector pDONR207 using Gateway cloning technology (Invitrogen, United States). *ZtWco-1* and *ZtWco-2* were then recombined into bait and prey vectors derived from pGADT7-GW and pGBKT7-GW plasmids. The bait and prey vectors were transformed into a yeast strain (Y2H Gold, Clontech) and grown on Trp and Leu drop-out medium (-TL) at 28 °C for 3 days. The yeast cells carrying both plasmids were then further selected on Trp/Leu/His/Ade drop-out medium (-TLHA). If ZTWCO-1 and ZTWCO-2 interact, yeast can grow on -TLHA plates at approximately 3–7 days. The experiment was repeated three times independently with two to three technical replicates per experiment.

#### 2.7. Construction of *ZtWco-1* knock-out vector

A knock-out vector for targeted deletion of *ZtWco-1* (p $\Delta$ ztwco-1) was constructed using yeast-based homologous recombination as outlined in Tiley et al. (2019). Briefly, the p $\Delta$ ztwco-1 vector consisted of a pCAM-BIA0380\_YA (yeast-adapted) backbone, the Hygromycin-*trpC* resistance cassette from pCB1003 (Carroll et al., 1994; Koay, 2010) and two 1.5 kb flanking regions targeting the *ZtWco-1* locus. The flanking regions were amplified with DreamTaq Green DNA Polymerase (Thermo Scientific) and the Hygromycin-*trpC* resistance cassette was amplified with Phusion® High-Fidelity DNA Polymerase (Thermo Scientific) using the manufacturer’s instructions. The primers used to construct the p $\Delta$ ztwco-1 vector are outlined in (Supporting Table 1).

The p $\Delta$ ztwco-1 DNA was recovered from *Saccharomyces cerevisiae* using Zymoprep™ Yeast Plasmid Miniprep II kit (Zymo Research). The vector was then transformed into *Escherichia coli* ccdB or DH5 $\alpha$  cells and isolated using the Gene JET Plasmid Miniprep Kit (Thermo Scientific) following the manufacturer’s instructions. Correct plasmid assembly was initially confirmed by PCR and further confirmed by sequencing, using the primers detailed in (Supporting Table 1).

#### 2.8. *Agrobacterium*-mediated transformation

The p $\Delta$ ztwco-1 knock-out vector was transformed into *A. tumefaciens* LBA1126 cells. *Agrobacterium*-mediated transformation was used to transform the *Z. tritici* IPO323 strain following the protocol outlined in Derbyshire et al. (2015) and Derbyshire et al. (2018). The authors acknowledge that complementation of the  $\Delta$ ztwco-1 mutants would strengthen this study. Complementation was attempted by outsourcing the synthetic generation of the  $\Delta$ ztwco-1-*comp* vector, but *ZtWco-1* could not be cloned. As a result, complementation of the  $\Delta$ ztwco-1 mutants was not feasible within the scope of this research.

#### 2.9. Confirmation of the $\Delta$ ztwco-1 mutants

Primary screening of the  $\Delta$ ztwco-1 knock-out mutants was carried out by growing the strains on YPDA agar (10 g/L yeast extract, 20 g/L

peptone, 20 g/L glucose and 20 g/L technical agar) supplemented with Hygromycin B (100 µg/ml) and Timentin™ (100 µg/ml). Potential mutants were then sub-cultured at least three times to single colonies. Successful deletion of the *ZtWco-1* gene was confirmed by PCR (Supporting Fig. 1). Wild-type and knock-out mutant fungal DNA was extracted using the protocol outlined in (Liu et al., 2000a). Double PCR was carried out using primer pairs to (1) amplify the wild-type *ZtWco-1* gene and (2) to confirm successful replacement of *ZtWco-1* with the Hygromycin-*trpC* resistance cassette. Primers used for knock-out confirmation are detailed in (Supporting Table 1).

## 2.10. In planta infections and virulence assays

Virulence of the *Z. tritici* strains was compared using attached wheat leaf inoculations, as described in Keon et al. (2007) and Tiley et al. (2018). Half-trays of the susceptible wheat cv. Riband were grown at 20 °C under 16:8 LD cycles until seedlings reached growth stage 12 – 13 (Tottman, 1987). The *Z. tritici* IPO323 isolate and  $\Delta ztwco-1$  mutant strains were grown on CDV8 under DD conditions at 20 °C for 3 – 5 days. The *Z. tritici* cells were suspended to a concentration of  $1 \times 10^6$  spores/ml in 0.01 % Tween 20. Wheat inoculations were performed at the same time of day, between 14 and 16 h of the 16:8 LD cycle. The first true leaf of each wheat seedling was attached adaxial side-up to polystyrene blocks using double-sided tape. A 10 cm section of each leaf was stroked three times using gloved hands to disrupt the waxy cuticle and promote infection. Each leaf was then swabbed ten times with a cotton bud dipped in the *Z. tritici* spore suspension. A 0.01 % Tween 20 solution was used as the negative control. Following infection, the plants were sealed inside a clear 40 µm thick autoclave bag and incubated in high humidity for 72 h at 20 °C under a 16:8 LD cycles. One half-tray containing 10 – 11 seedlings was infected per treatment and the experiment was repeated independently three times. All experiments were conducted between 12:00 – 14:00 and the infected plants were returned to the growth chamber no more than one hour before the start of the 8 h of darkness.

Comparison of virulence of the *Z. tritici*  $\Delta ztwco-1$  mutants and IPO323 strain was assessed by monitoring and recording disease progression every two days. Disease symptoms on the infected leaves were scored by visual observation on a scale from 1 to 5 (1 = no symptoms, 2 = chlorotic flecks, 3 = chlorosis, 4 = necrosis and 5 = pycnidia). Percentage leaf area covered in pycnidia (PLACP) was visually scored at 21 dpi using a modified scale based on Poppe et al. (2015), Zhan et al.

(2016) and Mohammadi et al. (2017). Disease levels were quantified using a scheme with 11 categories; 0 %, 10%, 20%, 30%, 40%, 50%, 60%, 70%, 80%, 90% and 100% PLACP. Scoring was carried out by the same person.

The wheat leaves were harvested at 21 dpi as described previously in Tiley et al. (2018). Representative 1 cm sections from each of the leaves were used to calculate pycnidia/mm<sup>2</sup>. A 5 cm section from each leaf was incubated on 4 layers of filter paper (Whatmann®) moistened with 5 ml SDW for 48 h under DD conditions at 20 °C (Derbyshire et al., 2015). The leaf sections were vortexed in 2 ml SDW for 15 s after which macro-pycnidiospores and micropycnidiospores were counted using a haemocytometer. The average number of macro-pycnidiospores per pycnidium and micropycnidiospores per pycnidium were calculated by dividing the number of macro-pycnidiospores or micropycnidiospores in the spore suspension by the number of pycnidia.

## 2.11. RNA extractions and RT-qPCR

The *Z. tritici* IPO323 strain and  $\Delta ztwco-1$  mutants were grown on CDV8 for three days under DD conditions at 20 °C. The cultures were exposed to white light for 15 min (Wu et al., 2014) and the fungal material was flash-frozen in liquid nitrogen. Approximately 100 mg of fungal material was harvested from two Petri dishes and pooled. The experiment was repeated independently three times. Total RNA was extracted using the Spectrum™ Total RNA Kit (Sigma-Aldrich) including On-Column DNase I Digestion (Sigma-Aldrich) following the manufacturer's instructions. Total RNA was quantified using a Nanodrop™ ND-1000 spectrophotometer (Thermo Scientific). Two cDNA reactions were synthesised from each RNA extraction. Reverse transcription of RNA was carried out using the Fermentas First Strand cDNA synthesis kit (Thermo Scientific) to yield 1 µg of cDNA.

Real-time quantitative PCR (RT-qPCR) was performed using Premix Ex Taq (Tli RNase H plus, RR420A; Takara) on a QuantStudio 7 Flex Real-Time PCR system (Applied Biosystems). Reactions were carried out in 12.5 µl volumes that included 1.25 µl of a 1:5 (v/v) dilution of cDNA, 0.2 µM of primers, and 1 × SYBR Premix Ex Taq (Tli RNase H plus, RR420A; Takara). PCR conditions were as follows: 1 cycle of 1 min at 95 °C; 40 cycles of 5 s at 95 °C and 20 s at 60 °C; and a final cycle of 1 min at 95 °C, 30 s at 55 °C, and 30 s at 95 °C for the dissociation curve. The *Mgtub* housekeeping gene (Rudd et al., 2015) and *ZtWco-1* and *ZtFrq* target gene primers are outlined in Supporting Table 1. Each template and primer combination was run once across three independent plates.

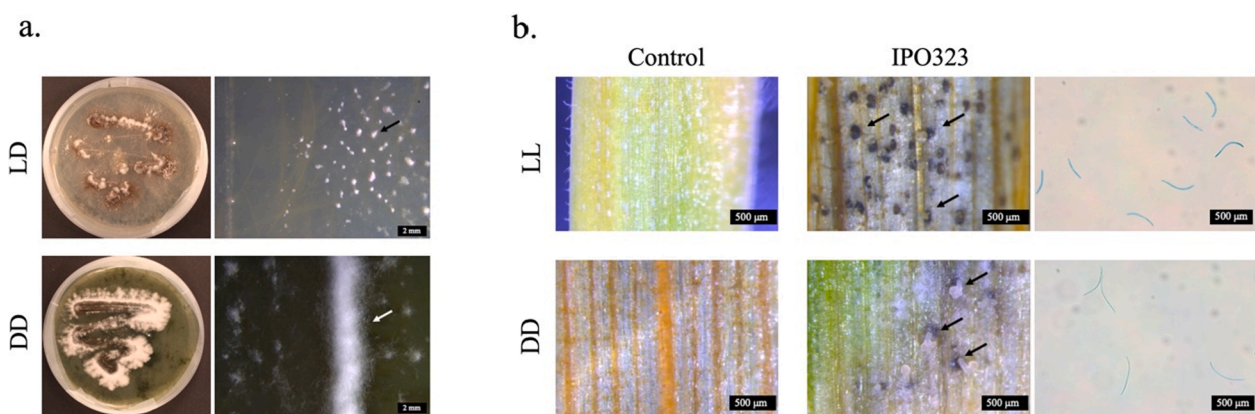


**Fig. 1. Impact of light on *Z. tritici* vegetative growth and asexual sporulation.** (a) *Z. tritici* IPO323 incubated on WEA under 12:12 light:dark (LD, WL) cycles and constant darkness (DD) at 20 °C. Cultures incubated under LD produce hyphal knots on the agar (black arrow). Cultures incubated under DD produce thick white aerial hyphal bands (white arrow). Images taken at 58 days post-inoculation and representative of three independent experiments with four Petri dishes incubated under each light condition; (b) detached wheat cv. Riband leaves inoculated with  $1 \times 10^6$  spores/ml *Z. tritici* IPO323 in 0.01% Tween 20 and incubated under continuous light (LL, WL-UVA) or DD. Leaves incubated under LL produce pycnidia (indicated by arrows) which ooze white cirrus containing pycnidiospores. Leaves incubated under DD conditions produce pycnidia (indicated by arrows) with white aerial hyphae which ooze white cirrus containing pycnidiospores. Images taken at 21 days post-inoculation and representative of two independent experiments with 3 – 4 Petri dishes containing 5 – 7 leaves tested per light condition.

The cycle threshold ( $\Delta Ct$ ) value was calculated and relative gene expression ( $Ct$  target gene –  $Ct$  housekeeping gene) as previously described (Livak and Schmittgen, 2001). The  $\Delta\Delta Ct$  value was calculated as ( $\Delta Ct$  targetgene -) and log-transformed to give the differences in relative transcript abundance ( $2^{-\Delta\Delta Ct}$ ).

### 2.12. Microscopy, photography and image analysis

*Z. tritici* spores and vegetative hyphae were stained with lactophenol cotton blue for analysis using light microscopy. Five  $\mu$ l of the stain was put on a glass microscope slide followed by 5  $\mu$ l of the fungal cell suspension and a cover slip. The specimen was left for 1 min before microscope analysis. Samples were observed using a Leica DM5500 B microscope or Leica M205 FA stereo microscope connected to a Leica DFC310 FX digital camera and captured using Leica Application Suite software V 4.4. Images of leaf samples were taken using a Canon EOS 100D camera with EF-S 18–55 mm f/3.5–5.6 IS STM Lens.

Measurements of fungal colony circumference were conducted using ImageJ (<https://imagej.nih.gov>, last accessed May 2022) and Fiji (Rueden et al., 2017; Schindelin et al., 2012; Schneider et al., 2012).

### 2.13. Statistical analyses

All statistical analyses were carried out using IBM SPSS Statistics 24 (IBM Corp., 2016). Data comparing colony area and pycnidia/ $\text{mm}^2$  followed a normal distribution and met the assumptions of Kolmogorov tests. A linear mixed effects model was used where either the mean colony area or pycnidia/ $\text{mm}^2$  was set as the dependent variable, fungal strain was set as the independent variable, and biological replicate was included as a random effect to account for variation between replicates. The assumption of homogeneity of variance was assessed using Levene's, Brown – Forsythe and Welch F tests. Tukey's honest significant difference (HSD) test at the 5 % significance level was used for post-hoc comparison between strains to account for multiple comparisons. The PLACP and the count data collected from the macropycnidiospores per pycnidium and micropycnidiospores per pycnidium analyses failed the assumption for the Kolmogorov tests and therefore did not follow a normal distribution. Outliers were removed from these datasets and an Independent Samples Kruskal-Wallis Pairwise Comparisons Test was used at the 5 % significance level, followed by Dunn's pairwise tests adjusted by the Bonferroni correction. The difference in relative transcript abundance ( $2^{-\Delta\Delta Ct}$ ) of *ZtFrq* also failed the assumption for the Kolmogorov tests. Therefore, the data was analysed by an Independent Samples Kruskal-Wallis Pairwise Comparisons Test at the 5 % significance level and Dunn's pairwise tests adjusted by the Bonferroni correction.

## 3. Results

### 3.1. Light impacts *Z. tritici* vegetative growth but is not essential for asexual sporulation

*Z. tritici* was grown *in vitro* on WEA under 12:12 light:dark (LD, WL) cycles and was compared to growth under constant darkness (DD). Under LD conditions, *Z. tritici* produced a thin layer of white aerial hyphae with white hyphal knots on the surface of the agar. In contrast, under DD conditions, *Z. tritici* produced a visibly thicker layer of white aerial hyphae on the agar surface (Fig. 1a). Pycnidia were observed under both LD and DD conditions on the WEA (Supporting Fig. 2). However, the pycnidia developed embedded within the agar and so extraction of the pycnidiospores was not attempted. The impact of light on asexual sporulation was evaluated further by infecting detached wheat leaves with *Z. tritici* and incubating under constant light (LL, WL-UVA) or DD conditions. Constant WL-UVA was used to promote pycnidia production *in vitro*. *Z. tritici* also produced pycnidia on detached leaves under both LL and DD conditions. The pycnidia produced cloudy cirrus

which contained pycnidiospores (Fig. 1b).

### 3.2. The genome of *Z. tritici* contains putative orthologs to the *N. Crassa* blue light photoreceptor genes *white collar-1* and *white collar-2*

FASTA protein sequences from *wc-1* and *wc-2* genes characterised in model ascomycete fungi were queried against the *Z. tritici* IPO323 genome database using the tblastn filtered models (transcripts) algorithm (<https://mycocosm.jgi.doe.gov/Mycgr3>, last accessed May 2022) (Goodwin et al., 2011). These analyses consistently identified the same seven candidates in *Z. tritici* as matches to the WHITE COLLAR-1 (WC-1) sequences queried. In addition, the same three candidates in *Z. tritici* were consistently identified as matches to the WHITE COLLAR-2 (WC-2) sequences queried. There was overlap between the *wc-1* and *wc-2* gene candidates identified in *Z. tritici*. The three matches to the WC-2 sequences queried were among the list of the seven WC-1 matches (Supporting Table 2; Supporting Table 3).

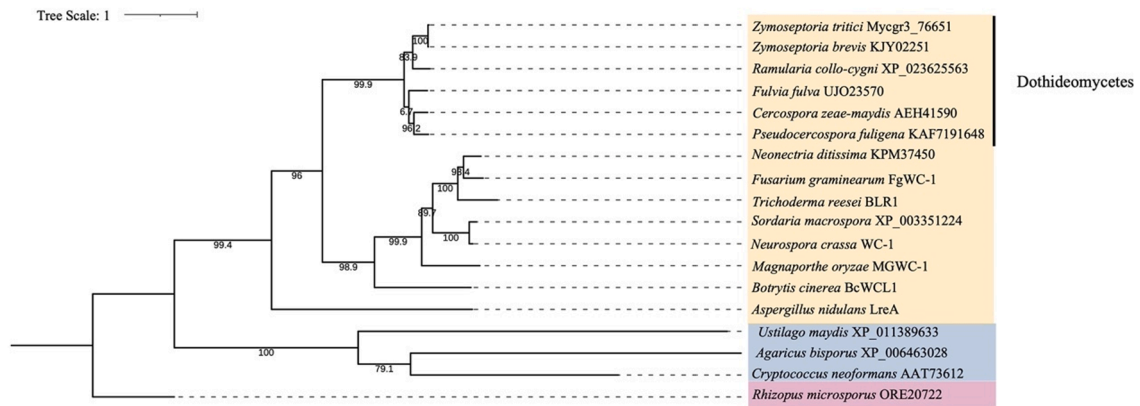
The *Z. tritici* Mycgr3\_76651 gene (GenBank® protein accession: XP\_003848281) was identified as the *wc-1* homolog in this species. The predicted Mycgr3\_76651 protein had the highest similarity against all of the fungal WC-1 protein sequences queried (Supporting Table 2). In addition, Best Bidirectional Blast Hit analysis confirmed Mycgr3\_76651 as the closest match to WC-1 proteins from five of the six model ascomycete species (Supporting Table 4). A maximum likelihood phylogenetic tree clustered the Mycgr3\_76651 protein with putative WC-1 proteins annotated in Dothideomycete plant pathogens (Fig. 2a), which is phylogenetically consistent with the species queried.

The Mycgr3\_76651 gene had previously been annotated as *MgWCO-1*, but we suggest re-naming to *ZtWco-1* in order to reflect the change in the nomenclature of this pathogen (Quaedvlieg et al., 2011). The *ZtWco-1* gene is predicted to be located on the *Z. tritici* core Chromosome 11 at position 222,416 – 225,920 and the transcript is 3, 238 base pairs in length. The hypothetical protein is 1, 068 amino acid residues in length, and it is predicted to contain three PAS domains and a single GATA-type zinc finger domain, which are characteristic of WC-1 proteins (Fig. 2b). The first PAS domain contains conserved regions typically associated with LOV domains. For example, the GxNCRFLQ submotif which has a cysteine that is critical for formation of the cysteinyl-flavin product (Fig. 2b; Supporting Table 3) (Glantz et al., 2016). Of the seven candidates identified, only Mycgr3\_76651 is predicted to encode a PAS domain containing the GxNCRFLQ submotif as well as a GATA-type zinc finger domain.

The *Z. tritici* Mycgr3\_32587 gene (GenBank® protein accession: XP\_003857660) was consistently the highest hit to the WC-2 FASTA sequences queried against the pathogen's genome (Supporting Table 2). Best Bidirectional Blast Hit analysis confirmed Mycgr3\_32587 as the closest match to four of the six WC-2 proteins from the model ascomycete species queried (Supporting Table 4). A maximum likelihood phylogenetic tree placed the Mycgr3\_32587 protein in a position that is phylogenetically consistent with the species queried (Fig. 3a).

The location of the *ZtWco-2* transcript is annotated on core chromosome 1 at location 1,215,964 – 1,217,445 and the protein is 493 amino acid residues in length. Manual inspection of the *ZtWco-2* gene structure led to the reannotation of *ZtWco-2* to location 1,215,874 – 1,217,445 (Supporting Table 3). The nucleotide sequence data reported are available in the Third Party Annotation Section of the DDBJ/ENA/GenBank databases under the accession number TPA: BK061372. The reannotated *ZtWco-2* gene is 1, 572 bp in length and it is predicted to encode 523 amino acid residues (Fig. 3). The hypothetical ZTWCO-2 protein is predicted to encode a single PAS domain and a GATA-type zinc finger domain which are characteristic of WC-2 proteins. Visual inspection of the predicted ZTWCO-2 amino acid sequence did not reveal the presence of a LOV domain or GxNCRFLQ submotif (Fig. 3; Supporting Table 3).

a.



b.

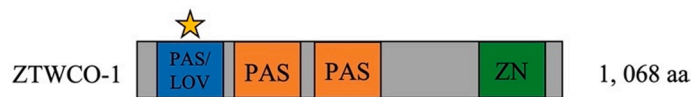
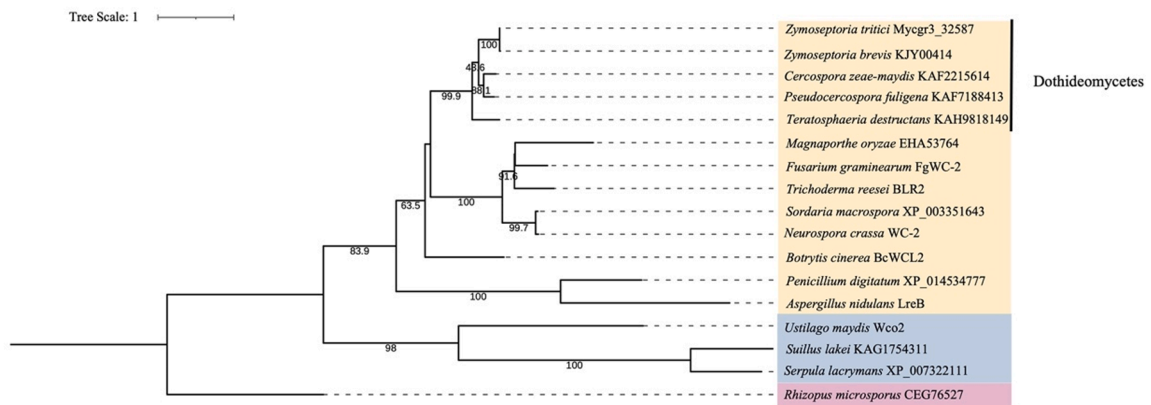


**Fig. 2. Identification of the *ZtWco-1* gene in *Z. tritici*.** (a) Maximum likelihood phylogenetic tree of WHITE COLLAR-1 (WC-1) proteins and their relatedness to Mycgr3\_76651. FASTA sequences were obtained from the NCBI database and aligned with Clustal W. The phylogenetic tree was generated using IQ-Tree and Model Finder with a bootstrap test at 1000 replicates. Visualisation was using iTOL with rooting on the Mucoromycota outgroup. Boxes represent fungal divisions, purple = Mucoromycota; blue = Basidiomycota and yellow = Ascomycota. Tree scale represents substitutions per site; (b) Schematic summarising the predicted protein structure for ZTWCO-1 following functional analysis of the FASTA sequences using InterProScan. These include the PAS/Light Oxygen Voltage domain (PAS/LOV), PAS domains (PAS), GATA-type zinc finger domain (ZN) and GxNCRFLQ submotif (star).

a.



b.



**Fig. 3. Identification of the *ZtWco-2* gene in *Z. tritici*.** (a) Maximum likelihood phylogenetic tree of WHITE COLLAR-1 (WC-2) proteins and their relatedness to Mycgr3\_32587. FASTA sequences were obtained from the NCBI database and aligned with Clustal W. The phylogenetic tree was generated using IQ-Tree and Model Finder with a bootstrap test at 1000 replicates. Visualisation was using iTOL with rooting on the Mucoromycota outgroup. Boxes represent fungal divisions, purple = Mucoromycota; blue = Basidiomycota and yellow = Ascomycota. Tree scale represents substitutions per site; (b) Schematic summarising the predicted protein structure for ZTWCO-2 following functional analysis of the FASTA sequences using InterProScan. This includes the PAS domain (PAS) and GATA-type zinc finger domain (ZN).

### 3.3. ZTWCO-1 and ZTWCO-2 may form a white collar complex

It has been previously reported that the WC-1 and WC-2 proteins interact with each other to form a white collar complex (WCC) in *Neurospora crassa* (He et al., 2002; Talora et al., 1999). Therefore, we tested whether this is also true in *Z. tritici* by using a combination of Protein 3D Structure & Function Prediction and yeast two-hybrid screening.

The highest scoring model produced by the I-TASSER server for ZTWCO-1 and ZTWCO-2 (c-score:  $-0.14$  and  $-2.18$  respectively) was subsequently chosen to visualise the 3D interaction complex of ZTWCO-1 and ZTWCO-2 using the ClusPro server (Desta et al., 2020; Kozakov et al., 2017, 2013; Vajda et al., 2017) (Fig. 4a and b).

In addition to exploring the 3D structure of ZTWCO-1 and ZTWCO-2, we examined possible Gene Ontology (GO) predictions for both proteins (Zhang et al., 2018). The highest scoring predictions for ZTWCO-1 was

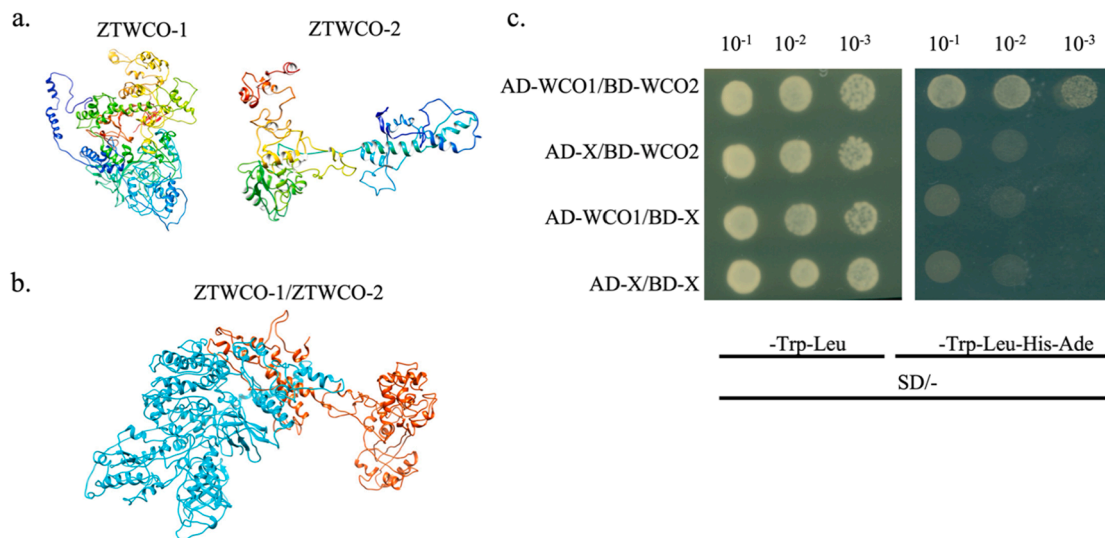


**Fig. 4.** Formation of the white collar complex in *Z. tritici*, (a) Representation of the 3D protein structure predicted by I-TASSER modelling for ZTWCO-1 and ZTWCO-2. Colours represent different chains within the 3D structure; (b) Representation of the 3D protein–protein interaction of WC-1 (cyan) and WC-2 (orange). Computation protein docking was produced by ClusPro; (c) image of yeast two-hybrid assay showing interaction between ZTWCO-1 and ZTWCO-2 proteins in yeast. The AD and BD represents the Gal4 activation domain and DNA binding domain respectively.

identified as compound binding and heterocyclic compound binding, with a score of 0.16 and 0.17 respectively. The highest scoring predictions for ZTWCO-2 was transcription factor activity, sequence-specific DNA binding and DNA binding, with a score of 0.33 and 0.30. These results suggest that both ZTWCO-1 and ZTWCO-2 have a predicted molecular function which is involved in binding activities.

The predicted interaction between the *Z. tritici* ZTWCO-1 and ZTWCO-2 proteins was tested using yeast two-hybrid assay. ZTWCO-1

and ZTWCO-2 were found to interact in yeast cells *in vitro*, suggesting possible formation of a white collar complex in *Z. tritici* (Fig. 4c).

#### 3.4. Generation of $\Delta ztwco-1$ knock-out mutants

The role of *ZtWco-1* in *Z. tritici* development and virulence was investigated by integrating the  $p\Delta ztwco-1$  transfer-DNA into *Z. tritici* IPO323 using *Agrobacterium*-mediated transformation. Successful

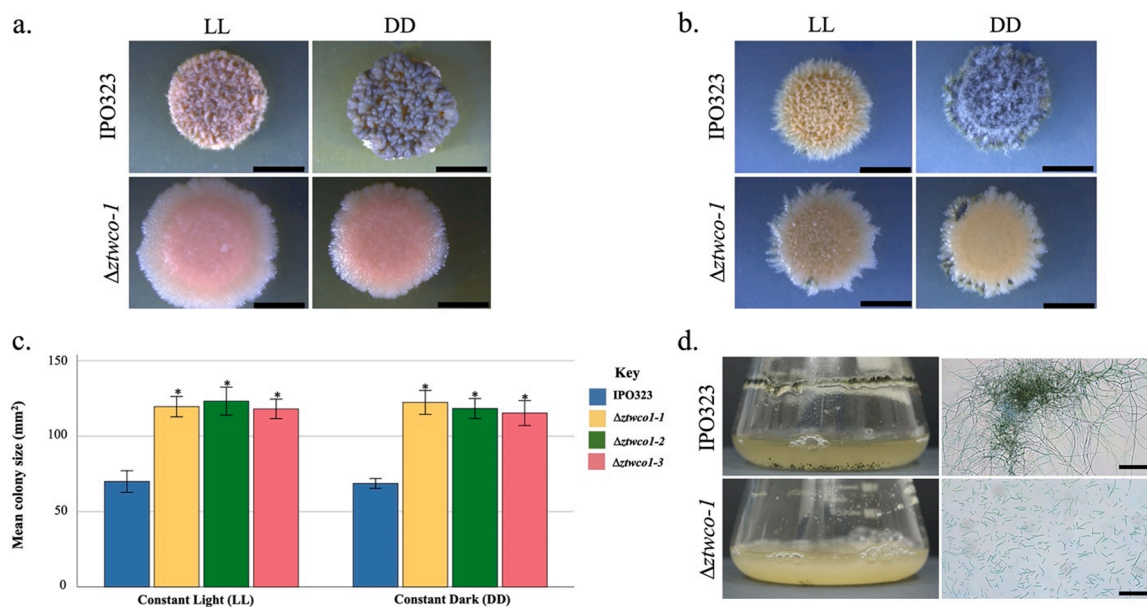


**Fig. 5.** Comparison of *Z. tritici* IPO323 and  $\Delta ztwco-1$  mutant growth on solid media and in liquid media, (a; b)  $1 \times 10^6$  spores/ml were plated on (a) YPDA and (b) PDA, and incubated under constant white light (LL) or constant darkness (DD) at 20 °C. Images taken at 14 days post-inoculation and representative of the three  $\Delta ztwco-1$  mutants tested against the IPO323 strain. Between 3 and 4 Petri dishes were analysed per strain under each media and each light condition. The experiment was repeated independently three times. Scale bar = 5 mm. Under LL conditions on YPDA and PDA the IPO323 colonies are yeast-like, but melanise and produce aerial hyphae under DD conditions. The  $\Delta ztwco-1$  mutants remain yeast-like in appearance with little or no melanisation under LL and DD conditions on YPDA and PDA; (c) Average colony area of the  $\Delta ztwco-1$  mutants is significantly larger than the IPO323 strain on YPDA under LL and DD conditions. Bars represent  $\pm 2$  standard error and an asterisk (\*) denotes significant difference to IPO323 (Tukey's honest significant difference test \* for  $p < 0.05$ ); (d) *Z. tritici* IPO323 and  $\Delta ztwco-1$  growth in liquid PDB at 200 rpm and 20 °C. Images taken at 7 dpi and representative of 2–3 flasks inoculated per strain across two independent experiments. Scale bar = 100  $\mu$ m. The IPO323 strain produces melanised hyphal knots, a melanised ring and branching hyphae in PDB. In contrast, the  $\Delta ztwco-1$  mutants produce small melanised hyphal knots and short yeast-like cells with minimal branching.

knock-out mutants with deletions in the *ZtWco-1* gene were purified by subculturing onto selective media containing Hygromycin B. PCR was performed using two primer pairs (Supporting Table 1) to confirm replacement of the wild-type *ZtWco-1* gene with the *hyg-trpC* cassette (Supporting Fig. 1). Three independent  $\Delta zt w c o - 1$  knock-out mutants ( $\Delta z t w c o - 1 - 1$ ,  $\Delta z t w c o - 1 - 2$  and  $\Delta z t w c o - 1 - 3$ ) were identified and used for all downstream experiments.

Further validation of the  $\Delta z t w c o - 1 - 1$ ,  $\Delta z t w c o - 1 - 2$  and  $\Delta z t w c o - 1 - 3$  mutant lines was performed by RT-qPCR to confirm deletion of *ZtWco-1*. Expression of *ZtWco-1* was not detected in  $\Delta z t w c o - 1 - 1$ ,  $\Delta z t w c o - 1 - 2$  or  $\Delta z t w c o - 1 - 3$ , therefore supporting evidence that the *ZtWco-1* gene had been deleted in all three of the mutant lines (Supporting Fig. 3).

### 3.5. *ZtWco-1* is required for light response in vitro

To assess the role of *ZtWco-1* in *Z. tritici* development, vegetative growth of the IPO323 parental strain and the  $\Delta z t w c o - 1$  mutants was compared *in vitro*. Experiments were carried out on PDA and YPDA under constant white light (LL) and constant darkness (DD) and images were taken at 7-, 14- and 21-days post-inoculation (dpi) (Fig. 5).

We previously recorded that the IPO323 strain melanises faster under DD conditions compared to LL conditions (Tiley et al., 2019). This was observed again, and by 14 dpi the IPO323 strain was melanised on both YPDA and PDA under DD conditions. On PDA under DD conditions, the IPO323 strain produced white aerial hyphae. IPO323 cultures incubated on PDA and YPDA under LL remained pink/peach in colour with little or no melanisation (Fig. 5a, b). In contrast to IPO323, there was no phenotypic difference between the  $\Delta z t w c o - 1$  mutants incubated under LL or DD conditions on either YPDA or PDA. The  $\Delta z t w c o - 1$  mutants remained pink/peach-coloured with little or no melanisation of the colonies (Fig. 5a, b).

The area of the IPO323 and  $\Delta z t w c o - 1$  mutant colonies grown on YPDA under LL and DD conditions after 14 dpi were compared to assess whether deletion of *ZtWco-1* affects growth rate. Under both LL and DD conditions, the colony area of the three  $\Delta z t w c o - 1$  mutants were significantly larger than the IPO323 strain. Under LL conditions, there was a statistical difference between the colony size of the IPO323 strain ( $n = 9$ ) compared to  $\Delta z t w c o - 1 - 1$  ( $n = 8$ , SE = 5.38, df = 69,  $p < 0.001$ ),  $\Delta z t w c o - 1 - 2$  ( $n = 8$ , SE = 5.38, df = 69,  $p < 0.001$ ) and  $\Delta z t w c o - 1 - 3$  ( $n = 8$ , SE = 5.38, df = 69,  $p < 0.001$ ). Under DD conditions, there was also a statistical difference between the colony size of the IPO323 strain ( $n = 11$ ) compared to  $\Delta z t w c o - 1 - 1$  ( $n = 11$ , SE = 4.7, df = 69,  $p < 0.001$ ),  $\Delta z t w c o - 1 - 2$  ( $n = 11$ , SE = 4.7, df = 69,  $p < 0.001$ ) and  $\Delta z t w c o - 1 - 3$  ( $n = 11$ , SE = 4.7, df = 69,  $p < 0.001$ ). (Fig. 5c).

There was no significant difference between the colony areas of the IPO323 strain when grown under LL ( $n = 11$ ) or DD conditions ( $n = 9$ , SE = 5.0, df = 69,  $p = 1.0$ ) (Fig. 5c). Similarly, there was no significant difference between the colony area of  $\Delta z t w c o - 1$  mutants grown under LL and DD conditions. This was  $\Delta z t w c o - 1 - 1$  LL ( $n = 8$ )  $\Delta z t w c o - 1 - 1$  DD ( $n = 11$ , SE = 5.1, df = 69,  $p = 1.0$ ),  $\Delta z t w c o - 1 - 2$  LL ( $n = 8$ )  $\Delta z t w c o - 1 - 2$  DD ( $n = 11$ , SE = 5.1, df = 69,  $p = 1$ ) and  $\Delta z t w c o - 1 - 3$  LL ( $n = 8$ )  $\Delta z t w c o - 1 - 3$  DD ( $n = 11$ , SE = 5.1, df = 69,  $p = 1.0$ ) (Fig. 5c).

### 3.6. *ZtWco-1* is essential for hyphal development

Further experiments were conducted to assess the role of *ZtWco-1* on cell morphology. The IPO323 strain and  $\Delta z t w c o - 1$  mutants were grown in PDB. Under these liquid cultivation conditions at 7 dpi, the parental IPO323 strain produced opaque peach-coloured cultures that contained melanised hyphal knots. In addition, the IPO323 strain produced a ring of hyphae around the edge of the flask. Microscopic observations demonstrated that the IPO323 cultures were composed of long hyphal branching cells, with few short yeast-like cells present. The  $\Delta z t w c o - 1$  mutants grew as opaque cultures, but there were few melanised hyphal knots visible and these strains did not form a ring of hyphae around the edge of the flask. Microscopy analyses of the  $\Delta z t w c o - 1$  mutant

demonstrated that, in contrast to the IPO323 cells, the mutant predominantly grew as short yeast-like cells approximately 50  $\mu\text{m}$  or less in size, with few or no branching cells present (Fig. 5d).

### 3.7. The $\Delta z t w c o - 1$ mutants have delayed infection on wheat

In order to assess the effect of deletion of *ZtWco-1* on virulence, the susceptible wheat cultivar Riband (Chartrain et al., 2004) was infected with the parental wild-type IPO323 strain and the three  $\Delta z t w c o - 1$  mutants. Disease progression was measured by scoring infection severity on a scale of 1–5 as described in Tiley et al. (2018) every 48 h for 21 days post-infection.

All three independent  $\Delta z t w c o - 1$  mutants were able to infect wheat, but the onset of chlorosis and necrosis were delayed by 2–4 days compared to the parental IPO323 strain (Fig. 6a, b). In addition, whereas the parental IPO323 strain produced pycnidia at approximately 13 dpi, the  $\Delta z t w c o - 1$  mutants did not produce pycnidia until 15–19 dpi (Fig. 6a, b).

### 3.8. The *ZtWco-1* gene impacts pycnidia numbers in planta

Although the  $\Delta z t w c o - 1$  mutants were able to produce normal symptoms on wheat, the disease progression was delayed compared to the IPO323 strain and this could impact virulence potential. In order to investigate this further, final measurements of percentage leaf area covered by pycnidia (PLACP) was recorded at 21 dpi. These results demonstrate that the  $\Delta z t w c o - 1$  mutants produced a smaller PLACP compared to the IPO323 strain. There was a statistical difference between the PLACP recorded for the IPO323 strain ( $n = 34$ ) compared to  $\Delta z t w c o - 1 - 1$  ( $n = 32$ , SE = 9.36, df = 131,  $p < 0.001$ ),  $\Delta z t w c o - 1 - 2$  ( $n = 34$ , SE = 9.22, df = 131,  $p < 0.001$ ) and  $\Delta z t w c o - 1 - 3$  ( $n = 35$ , SE = 9.15, df = 131,  $p < 0.001$ ) (Fig. 7a).

This result was investigated further by calculating the number of pycnidia produced/ $\text{mm}^2$ . All three of the  $\Delta z t w c o - 1$  mutants had a reduction in pycnidia/ $\text{mm}^2$  compared to the IPO323 strain and this was statistically significant at the 5 % level. There was a significant difference in the number of pycnidia/ $\text{mm}^2$  produced by the IPO323 strain ( $n = 31$ ) compared to  $\Delta z t w c o - 1 - 1$  ( $n = 31$ , SE = 0.30, df = 120,  $p < 0.001$ ),  $\Delta z t w c o - 1 - 2$  ( $n = 32$ , SE = 0.30, df = 120,  $p < 0.001$ ) and  $\Delta z t w c o - 1 - 3$  ( $n = 30$ , SE = 0.30, df = 120,  $p < 0.001$ ) (Fig. 7b).

Microscopy analyses did not reveal any phenotypic differences between pycnidia melanisation or morphology. The pycnidia produced by both the IPO323 strain and  $\Delta z t w c o - 1$  mutants were round, melanised, and embedded within the leaf sub-stomatal cavity (Fig. 7c).

### 3.9. The *ZtWco-1* gene represses micropycnidiospore production

We have previously demonstrated that the *Z. tritici* IPO323 strain is capable of producing both macropycnidiospores and micropycnidiospores *in planta*, and that both of these spore types can infect wheat (Tiley et al., 2019). Microscopy analyses on spore suspensions obtained from the infected wheat leaves demonstrated that the  $\Delta z t w c o - 1$  mutants and IPO323 strain produced both macropycnidiospores and micropycnidiospores. The average number of macropycnidiospores and micropycnidiospores produced per pycnidium by the  $\Delta z t w c o - 1$  mutants were compared to the IPO323 strain to determine whether deletion of *ZtWco-1* impacts asexual sporulation capacity. There was no significant difference between the average number of macropycnidiospores per pycnidium produced by the IPO323 strain ( $n = 30$ ) compared to  $\Delta z t w c o - 1 - 1$  ( $n = 30$ , SE = 8.7, df = 114,  $p > 0.05$ ),  $\Delta z t w c o - 1 - 2$  ( $n = 30$ , SE = 8.6, df = 114,  $p > 0.05$ ) and  $\Delta z t w c o - 1 - 3$  ( $n = 28$ , SE = 8.8, df = 114,  $p > 0.05$ ) (Fig. 8a). However, the IPO323 strain ( $n = 28$ ) produced significantly fewer micropycnidiospores per pycnidium compared to  $\Delta z t w c o - 1 - 1$  ( $n = 26$ , SE = 9.0, df = 110,  $p < 0.001$ ),  $\Delta z t w c o - 1 - 2$  ( $n = 30$ , SE = 8.7, df = 110,  $p < 0.001$ ) and  $\Delta z t w c o - 1 - 3$  ( $n = 30$ , SE = 8.7, df = 110,  $p < 0.001$ ) (Fig. 8b). Although there were significant

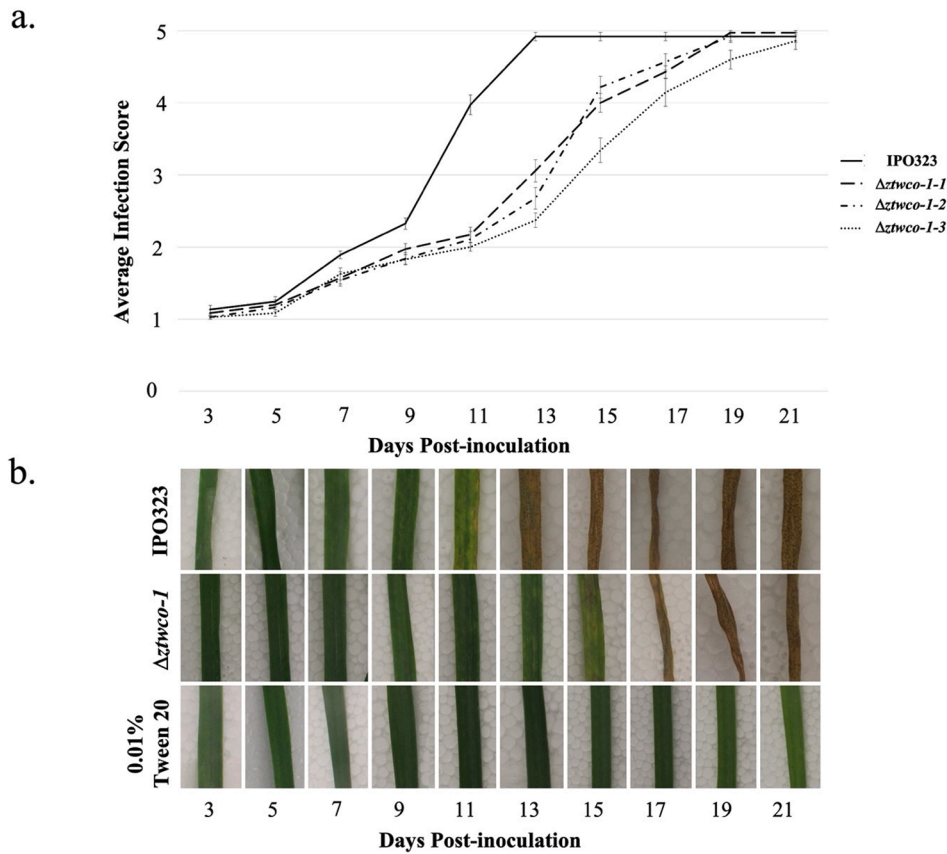


**Fig. 6.** Infection of wheat cv. Riband by *Z. tritici* IPO323 compared to the  $\Delta ztwco-1$  mutants, Wheat cv. Riband was infected with *Z. tritici* IPO323 and the  $\Delta ztwco-1$  mutants, and infection progression was recorded at 3 – 21 days post-inoculation (dpi). Between 10 and 11 leaves were analysed per strain and the experiment was repeated three times independently. Bars represent  $\pm 2$  standard error. Images are representative of the three  $\Delta ztwco-1$  mutants tested against the IPO323 strain. (a) the  $\Delta ztwco-1$  mutants produce the same sequence of symptoms as the parental IPO323 strain, but disease progression is slower; (b) representative images of wheat infection from 3 to 21 dpi.

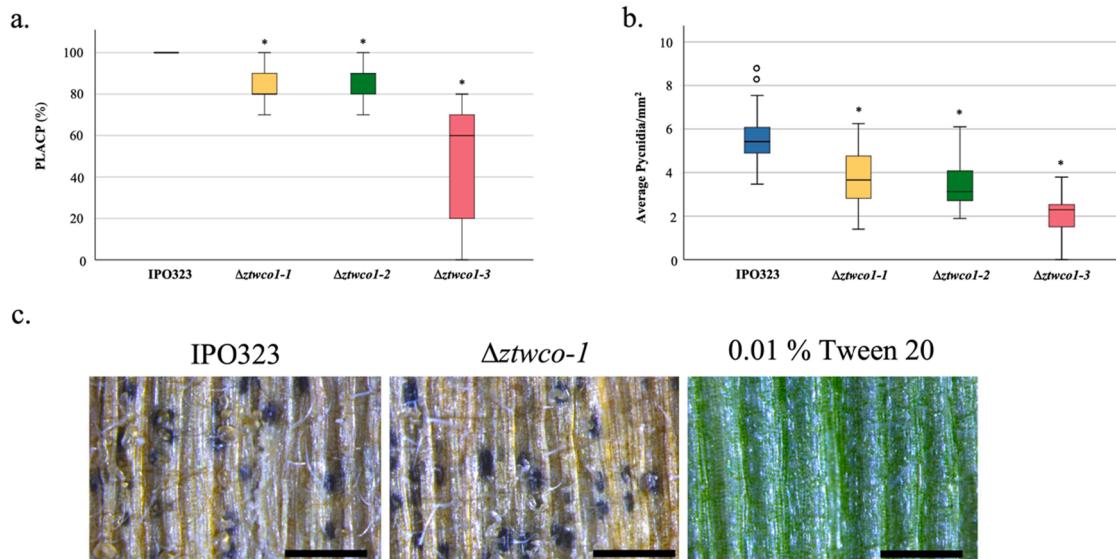


**Fig. 7.** Comparison of pycnidia produced on wheat by the  $\Delta ztwco-1$  mutants compared to the IPO323 strain, The percentage leaf area covered in pycnidia (PLACP), pycnidia/mm<sup>2</sup> and pycnidia morphology were compared on wheat cv. Riband at 21 days post-inoculation. Between 10 and 11 leaves were analysed per strain and the experiment was repeated three times independently. Bars represent  $\pm 2$  standard error and asterisks (\*) signify  $\Delta ztwco-1$  mutants significantly different to the IPO323 strain. Images are representative of the three  $\Delta ztwco-1$  mutants tested against the IPO323 strain. (a) PLACP at 21 dpi is significantly reduced in the three  $\Delta ztwco-1$  mutants compared to the IPO323 strain (Independent Samples Kruskal-Wallis Pairwise Comparisons Test \* for  $p < 0.001$ ); (b) all three  $\Delta ztwco-1$  mutants produce significantly fewer pycnidia/mm<sup>2</sup> than the IPO323 strain (Tukey's honest significant difference test \* for  $p < 0.001$ ); (c) There is no observable difference between the pycnidia produced by the three  $\Delta ztwco-1$  mutants compared to the IPO323 strain. Scale bar = 500  $\mu$ m.

differences between micropycnidiospore per pycnidium production, our microscopy analyses did not reveal any phenotypic differences between the morphology of either the macropycnidiospores or micropycnidiospores produced by the  $\Delta ztwco-1$  mutants compared to the

parental IPO323 strain (Fig. 8c).

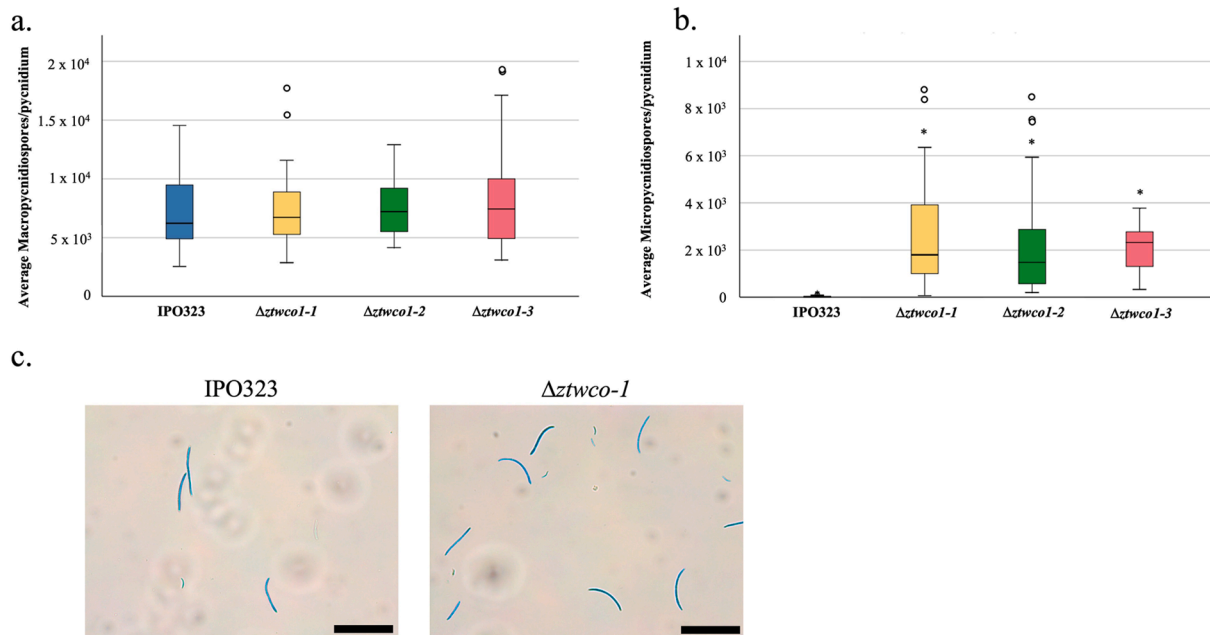


**Fig. 8. Comparison of asexual sporulation between the  $\Delta ztwco-1$  mutants and IPO323 strain.** Macropycnidiospore and micropycnidiospore production and morphology was compared on wheat cv. Riband at 21 days post-inoculation. Between 10 and 11 leaves were analysed per strain and the experiment was repeated three times independently. Bars represent  $\pm 2$  standard error and an asterisk (\*) signifies  $\Delta ztwco-1$  mutants significantly different to the IPO323 strain. Images are representative of the three  $\Delta ztwco-1$  mutants tested against the IPO323 strain. (a) There is no significant difference between the macropycnidiospores produced per pycnidium by the three  $\Delta ztwco-1$  mutants compared to the IPO323 strain (Independent Samples Kruskal-Wallis Pairwise Comparisons Test); (b) However, the three  $\Delta ztwco-1$  mutants produce significantly more micropycnidiospores per pycnidium than the IPO323 strain (Independent Samples Kruskal-Wallis Pairwise Comparisons Test \* for  $p < 0.001$ ); (c) There is no observable difference between the macropycnidiospores or micropycnidiospores produced by the three  $\Delta ztwco-1$  mutants compared to the IPO323 strain. Scale bar = 50  $\mu m$ .

### 3.10. The *Z. Tritici* genome contains a putative homolog to the *N. Crassa* frequency gene

*In silico* analyses were conducted in order to identify the *Z. tritici* homolog to the *N. crassa* *frq* gene (*ZtFrq*). The FASTA sequences of FRQ proteins from model ascomycete fungi were queried against the *Z. tritici* IPO323 genome database as described previously. The analyses consistently identified the *Z. tritici* Mycgr3\_93972 gene (GenBank® accession: XP\_003851799) as the only putative homolog to *frq* in the *Z. tritici* genome, and this was named *ZtFrq* (Supporting Table 2). The *ZtFrq* gene is predicted to be 3,015 base pairs in length and located on the *Z. tritici* core Chromosome 6 at position 1649–16–1652530. The hypothetical ZTFRQ protein is 1,004 amino acid residues in length. Functional analysis of the ZTFRQ FASTA sequence using InterProScan matched it to the frequency clock protein family. In addition, the ZTFRQ FASTA sequence contains regions similar to those characterised in the *N. crassa* FRQ protein. These include the conserved serine a position 513, which is a determinant of period length (Supporting Fig. 4) (Liu et al., 2000b).

RT-qPCR was performed on *in vitro* CDV8 cultures to elucidate whether expression of *ZtFrq* differs in the  $\Delta ztwco-1$  mutants compared to the wild-type IPO323 strain following a 15 min transition from darkness to white light (Wu et al., 2014). There was a significant difference in the relative transcript abundance of *ZtFrq* between the IPO323 strain ( $n = 6$ ) compared to  $\Delta ztwco-3$  ( $n = 6$ , SE = 4.08, df = 23,  $p = 0.016$ ). However, there was no significant difference in the relative transcript abundance of *ZtFrq* between the IPO323 strain and  $\Delta ztwco-1$  ( $n = 6$ , SE = 4.08, df = 23,  $p = 1.00$ ) or  $\Delta ztwco-2$  ( $n = 6$ , SE = 4.08, df = 23,  $p = 0.07$ ) (Supporting Fig. 4).

## 4. Discussion

In this study we further understanding of the genetic regulation of

light detection by *Z. tritici* and the role of the putative white collar-1 homolog, *ZtWco-1*. Previous studies suggest that *Z. tritici* can detect light and that this signal affects both growth and virulence (Fellows, 1962; Keon et al., 2007; Tiley et al., 2019; McCorison and Goodwin, 2020). However, the genetic basis of how *Z. tritici* detects light has not been previously studied in detail.

Growth on WEA demonstrates that *Z. tritici* can respond to light and dark conditions, and that this impacts development of aerial hyphae. These results are consistent with our previous findings as well as recent RNAseq data demonstrating that *Z. tritici* gene expression is affected by different light wavelengths (Tiley et al., 2019; McCorison and Goodwin, 2020). However, our detached leaf assays demonstrate that light is not essential for infection of wheat or the ability to undergo asexual sporulation. The result agrees with previous studies demonstrating that darkness reduces infection and that it slows development (Fellows, 1962; Keon et al., 2007). The finding may be supported by evidence that penetration of the wheat stomata by *Z. tritici* is random rather than determined by specific cues (Kema et al., 1996; Fones et al., 2017). Similarly to *Z. tritici*, the maize pathogen *C. zea-maydis* also infects the host via the stomata. However, *C. zea-maydis* displays stomatal tropism and light is necessary for successful detection of the stomata (H. Kim et al., 2011). Therefore, although *Z. tritici* can respond to light and dark, this signal may not be essential for virulence due to the manner in which this pathogen detects and infects its host.

The *Z. tritici* genome contains putative homologs to photoreceptors from other fungi including the two white collar complex genes (*wc-1* and *wc-2*), *VIVID*, a blue-light sensing cryptochrome, and a phytochrome (McCorison and Goodwin, 2020). In order to identify possible genetic regulators of light detection in *Z. tritici* we focused on the white collar photoreceptors which are highly conserved across the fungal kingdom. The results from our *in vitro* studies suggest that *ZtWco-1* is involved in perception and response to light and/or dark conditions. The IPO323 strain melanises under DD conditions on PDA and YPDA, suggesting that

light and/or dark conditions influence melanisation in *Z. tritici*. In contrast to IPO323, the phenotype of the  $\Delta ztwco-1$  mutant colonies did not differ under either LL or DD conditions. Melanisation was severely impaired in the  $\Delta ztwco-1$  mutants and so *ZtWco-1* may play a role in regulating melanin production. Light has previously been associated with melanin production in *M. oryzae*, and genes linked to melanin biosynthesis are differentially expressed during a light-to-dark transition (S. Kim et al., 2011). RNAseq data from *Z. tritici* previously highlighted that light conditions impact the expression of the mitogen-activated protein kinase (MAPK)-encoding genes *MgHog1* and *MgSlr2*, which both have roles in melanin production and virulence (McCorison and Goodwin, 2020). However, it is unlikely that melanisation is linked to virulence in *Z. tritici*. A previous study by Derbyshire et al. (2018) demonstrated that *Z. tritici* mutants with deletion of the polyketide synthase gene, *ZtPks1*, were unable to melanise on YPD agar. The  $\Delta ZtPks1$  mutants were able to infect wheat and they produced non-melanised pycnidia *in planta* (Derbyshire et al., 2018). In addition, deletion of the *Z. tritici* *velvet* gene, *MVE1*, resulted in albino mutants that had no difference in virulence on wheat and produced lightly coloured pycnidia *in planta* (Choi and Goodwin, 2011).

Although melanisation may not be essential for virulence in *Z. tritici*, it could be linked to vegetative growth. For example, some aspects of the *in vitro* phenotype observed in the  $\Delta ztwco-1$  mutants are also similar to that of *Z. tritici* *ZtVf* mutants (Mohammadi et al., 2017). The *ZtVf* gene is a member of the zinc-finger transcription factor family and deletion causes defects in hyphal filamentation and melanisation *in vitro*. We previously demonstrated that *Z. tritici* mutants with deletions in the *ZtvelB* gene are fixed in a filamentous growth pattern and melanise under both light and dark conditions (Tiley et al., 2019). Therefore, crossover may exist between the genetic pathways regulating pigmentation and hyphal branching in *Z. tritici*.

In liquid media, the  $\Delta ztwco-1$  mutants produced short yeast-like cells that formed few branched hyphae and few hyphal knots. This short unbranched cell phenotype was only observed in vegetative cells, as there were no visible differences between the IPO323 and  $\Delta ztwco-1$  mutant macropycnidiospores produced *in planta*. One possibility for the phenotype observed in the vegetative cells of the  $\Delta ztwco-1$  mutants is that deletion of *ZtWco-1* causes disordered growth which prevents hyphal aggregation. We have previously observed that hyphal knots are required for pycnidia formation (Tiley, 2016). Therefore, defects in hyphal aggregation may reduce or delay pycnidia production as observed in our *in planta* results.

Light and dark conditions have been shown to impact the outcome of plant pathogen interactions by affecting the plant defence response and/or pathogen virulence. For example, *A. thaliana* has decreased susceptibility to *B. cinerea* when the infection occurs at dawn compared to dusk (Hevia et al., 2015; Ingle et al., 2015). In addition, light has been shown to repress *M. oryzae* infection of rice (S. Kim et al., 2011). Previous studies have provided varying evidence for the role of light and darkness in *Z. tritici* infection of wheat. For example, infection is greatly reduced by darkness and shading leaves can slow the progression of symptom development (Fellows, 1962; Keon et al., 2007). However, light has also been shown to inhibit the early stages of infection but stimulate infection later on (Shaw, 1991). Comparison of *in planta* infections of wheat in this study demonstrated that symptom development is delayed by 2–4 days in the  $\Delta ztwco-1$  mutants compared to the wild-type IPO323 strain. This agrees with previous data from *B. cinerea* where *bcwcl1* deletion mutants produced smaller lesions on French bean (*Phaseolus vulgaris*) early during infection, but the mutants were still able to proceed to colonise and sporulate on the plant (Canessa et al., 2013). The delayed symptom development observed during this study could be caused by the defects in vegetative growth observed in the  $\Delta ztwco-1$  mutants. Fones et al. (2017) suggest that the hyphal form of *Z. tritici* is more adept at covering distance across the leaf surface. Hyphal differentiation is disrupted in the  $\Delta ztwco-1$  mutants, and this could delay successful stomatal penetration events and tissue colonisation. Although

our results suggest that the *ZtWco-1* gene is required for full virulence on wheat, the exact role in virulence remains to be elucidated.

Our results demonstrate that symptom progression was delayed in the  $\Delta ztwco-1$  mutants, but deletion of *ZtWco-1* does not affect pycnidia morphology. The pycnidia produced by the  $\Delta ztwco-1$  were melanised, which was unexpected considering that the  $\Delta ztwco-1$  mutant vegetative cells have defects in melanisation *in vitro*. In *B. cinerea*, three different types of melanin have been suggested that are tightly controlled at different developmental stages; mycelial, sclerotial and conidial (Schumacher, 2016). Therefore, our results suggest that *Z. tritici* may employ separate genetic pathways to regulate mycelial and pycnidial melanisation.

The role of *white collar-1* genes in asexual sporulation has been demonstrated in fungal species such as *A. nidulans*, *C. zea-maydis*, *F. graminearum* and *B. cinerea* (Canessa et al., 2013; H. Kim et al., 2011; Kim et al., 2014; Purschwitz et al., 2008). Deletion of *ZtWco-1* significantly reduced PLACP and pycnidia/mm<sup>2</sup> in the  $\Delta ztwco-1$  mutants compared to the wild-type IPO323 strain at 21 dpi. These results suggest that *ZtWco-1* may play a role in asexual sporulation. Although there was no significant difference in the macropycnidiospores produced per pycnidium between the  $\Delta ztwco-1$  mutants and the IPO323 strain, the  $\Delta ztwco-1$  mutants produced significantly more micropycnidiospores per pycnidium. The observed increase in micropycnidiospore production agrees with previous findings from the plant pathogens *C. zea-maydis*, *F. graminearum* and *B. cinerea*, where disruption of the *wc-1* homologs caused de-repression of conidiation (Canessa et al., 2013; H. Kim et al., 2011; Kim et al., 2014). We previously demonstrated that deletion of the *ZtvelB* gene impacts macropycnidiospore production but not micropycnidiospore production (Tiley et al., 2019). Therefore, it is possible that two separate genetic pathways regulate formation of these two different asexual spore types. The results observed in this study may also be a product of the delay in symptom progression observed in the  $\Delta ztwco-1$  mutants. For example, macropycnidiospore production and micropycnidiospore production may occur at separate stages of asexual sporulation rather than at the same time. Micropycnidiospore production may peak during the initial stages of asexual sporulation, which is typically 13 dpi onwards in the IPO323 strain, and at 19 dpi onwards in the  $\Delta ztwco-1$  mutants. Therefore, sampling at 21 dpi may only capture peak micropycnidiospore production in the  $\Delta ztwco-1$  mutants. Our results therefore demonstrate that loss of *ZtWco-1* attenuates infection of wheat by *Z. tritici*, but further studies are required to clarify the exact role of this gene in asexual sporulation.

Circadian clocks are entrained by environmental signals such as light, and our *in vitro* results demonstrate that *Z. tritici* can respond to this signal. In this study, we also identified putative homologs in *Z. tritici* to each of the *N. crassa* core circadian components: *wc-1*, *wc-2* and *frq*. In other ascomycete fungi, deletion of *wc-1* can impact *frq* expression. For example, Crosthwaite et al. (1997) reported an increase in the *N. crassa* *frq* transcript following a 2-minute pulse of white light in the wild-type strain. However, *frq* expression was not induced by a 2-minute pulse of white light in *wc-1* mutants (Crosthwaite et al., 1997). In *B. cinerea*, the absence of BCWL1 disrupts *bcfrq* oscillations (Hevia et al., 2015). Canessa et al. (2013) demonstrated that a transition from dark to light strongly induces relative expression of *bcfrq* in the wild-type strain, but this was not observed in the  $\Delta bcwcl1$  mutants. Our results were inconclusive as *ZtFrq* expression was only significantly different between the IPO323 strain and the  $\Delta ztwco1-3$  mutant. We therefore suggest that the *Z. tritici* IPO323 genome contains the genetic components for a functioning circadian clock, but it is not clear whether these components interact. Previous research on the plant pathogen *Verticillium dahliae* found no evidence for rhythmicity despite the presence of putative homologs to *wc-1*, *wc-2* and *frq* (Cascant-Lopez et al., 2020). Therefore, further studies are required to establish whether *Z. tritici* has a functioning circadian clock and, if so, whether *ZtWco-1*, *ZtWco-2* and *ZtFrq* are components of it.

## 5. Conclusions

This study characterises the putative photoreceptor in *Z. tritici*, *ZtWco-1*. We demonstrate that *ZtWco-1* may regulate light detection in *Z. tritici* and the control of downstream developmental processes such as melanisation, hyphal morphology, virulence and asexual sporulation on wheat. Findings from this study open multiple avenues of research into the role of light and the possibility of the presence of a circadian clock in *Z. tritici*. Understanding whether *Z. tritici* can detect light and the time of day may inform strategies future control strategies against this pathogen.

## CRedit authorship contribution statement

**Anna M.M Tiley:** Conceptualization, Methodology, Validation, Formal analysis, Investigation, Resources, Data curation, Writing – original draft, Writing – review & editing, Visualization, Project administration, Funding acquisition. **Colleen Lawless:** Methodology, Validation, Formal analysis, Investigation, Visualization, Writing – original draft, Writing – review & editing. **Paola Pilo:** Investigation, Validation, Writing – review & editing. **Sujit Karki:** Methodology, Validation, Formal analysis, Investigation, Visualization, Supervision, Writing – original draft, Writing – review & editing. **Jijun Lu:** Investigation, Validation. **Zhuowei Long:** Investigation, Validation. **Hesham Gibriel:** Methodology, Formal analysis, Investigation, Validation, Writing – original draft, Writing – review & editing. **Andy M. Bailey:** Resources, Supervision, Writing – review & editing, Funding acquisition. **Angela Feechan:** Resources, Supervision, Writing – review & editing.

## Declaration of Competing Interest

The authors declare that they have no known competing financial interests or personal relationships that could have appeared to influence the work reported in this paper.

## Acknowledgements

We thank Flora Greville for assistance with construction of the p*Δztwco-1* vector. The authors would also like to thank Dr Harriet Benbow for support with the bioinformatic analyses, and Dr Anthony Twamley for assistance with the RT-qPCR.

## Contributions

AMMT designed the project, performed the experiments, analysed the data, and wrote the manuscript. CL and PP assisted in conducting the RT-qPCR experiments. CL performed protein 3D structure and function predictions of ZTWCO-1 and ZTWCO-2 protein interactions. SJK, JL and ZL conducted the yeast two-hybrid assays. HG carried out visual inspection of the *ZtWco-1*, *ZtWco-2* and *ZtFrq* sequences. AMB provided the IPO323 and *Δztwco-1* strains as well as feedback on the manuscript. AF contributed to the experimental design, analysis and provided feedback on the manuscript.

## Funding Sources

AMMT was supported by a Government of Ireland Postdoctoral Fellowship Programme award (GOIPD/2018/461) and the BBSRC SWBio Doctoral Training Partnership. This work was performed under DEFRA licence number 51046-198767 and EPA GMO Register No. G0555-01 and G0647-01.

## Appendix A. Supplementary material

Supplementary data to this article can be found online at <https://doi.org/10.1016/j.fgb.2022.103715>.

## References

- Arraiano, L.S., Brading, P.A., Brown, J.K.M., 2001. Detached leaf assay *Mycosphaerella graminicola* (anamorph *Septoria tritici*) in wheat. *Plant Pathol.* 50, 339–346. <https://doi.org/10.1046/j.1365-3059.2001.00570.x>.
- Baker, C.L., Loros, J.J., Dunlap, J.C., 2012. The circadian clock of *Neurospora crassa*. *FEMS Microbiol. Rev.* 36 (1), 95–110. <https://doi.org/10.1111/j.1574-6976.2011.00288.x>.
- Ballario, P., Talora, C., Galli, D., Linden, H., Macino, G., 1998. Roles in dimerization and blue light photoresponse of the PAS and LOV domains of *Neurospora crassa* white collar proteins. *Mol. Microbiol.* 29 (3), 719–729. <https://doi.org/10.1046/j.1365-2958.1998.00955.x>.
- Ballario, P., Vittorioso, P., Magrelli, A., Talora, C., Cabibbo, A., Macino, G., 1996. White collar-1, a central regulator of blue light responses in *Neurospora*, is a zinc finger protein. *EMBO J.* 15 (7), 1650–1657.
- Benedict, W.G., 1971. Differential effect of light intensity on the infection of wheat by *Septoria tritici* Desm. under controlled environmental conditions. *Physiol. Plant Pathol.* 1 (1), 55–66. [https://doi.org/10.1016/0048-4059\(71\)90040-3](https://doi.org/10.1016/0048-4059(71)90040-3).
- Blum, M., Chang, H.Y., Chuguransky, S., Grego, T., Kandasamy, S., Mitchell, A., Nuka, G., Paysan-Lafosse, T., Qureshi, M., Raj, S., Richardson, L., Salazar, G.A., Williams, L., Bork, P., Bridge, A., Gough, J., Haft, D.H., Letunic, I., Marchler-Bauer, A., Mi, H., Natale, D.A., Necci, M., Orengo, C.A., Pandurangan, A.P., Rivoire, C., Sigrist, C.J.A., Sillitoe, I., Thanki, N., Thomas, P.D., Tosatto, S.C.E., Wu, C.H., Bateman, A., Finn, R.D., 2021. The InterPro protein families and domains database: 20 years on. *Nucleic Acids Res.* 49, D344–D354. <https://doi.org/10.1093/nar/gkaa977>.
- Bodenhofer, U., Bonatesta, E., Horejs-Kainrath, C., Hochreiter, S., 2015. msa: an R package for multiple sequence alignment. *Bioinformatics* 31 (24), 3997–3999. <https://doi.org/10.1093/bioinformatics/btv494>.
- Canessa, P., Schumacher, J., Hevia, M.A., Tudzynski, P., Larrondo, L.F., Freitag, M., 2013. Assessing the effects of light on differentiation and virulence of the plant pathogen *Botrytis cinerea*: Characterization of the White Collar complex. *PLoS ONE* 8 (12), e84223. <https://doi.org/10.1371/journal.pone.0084223>.
- Carroll, A.M., Sweigard, J.A., Valent, B., 1994. Improved vectors for selecting resistance to Hygromycin. *Fung. Genet. Rep.* 41 (1), 22. <https://doi.org/10.4148/1941-4765.1367>.
- Cascan Lopez, E., Crosthwaite, S.K., Johnson, L.J., Harrison, R.J., 2020. No evidence that homologs of key circadian clock genes direct circadian programs of development or mRNA abundance in *Verticillium dahliae*. *Front. Microbiol.* 11 (1977), 1–21. <https://doi.org/10.3389/fmicb.2020.01977>.
- Chartrain, L., Brading, P.A., Widdowson, J.P., Brown, J.K.M., 2004. Partial resistance to *Septoria Tritici Blotch* (*Mycosphaerella graminicola*) in wheat cultivars Arina and Riband. *Phytopathology* 94 (5), 497–504. <https://doi.org/10.1094/PHYTO.2004.94.5.497>.
- Choi, Y.-E., Goodwin, S.B., 2011. *MVE1*, encoding the velvet gene product homolog in *Mycosphaerella graminicola*, is associated with aerial mycelium formation, melanin biosynthesis, hyphal swelling, and light signalling. *Appl. Environ. Microbiol.* 77 (3), 942–953. <https://doi.org/10.1128/AEM.01830-10>.
- Corrochano, L.M., 2019. Light in the fungal world: from photoreception to gene transcription and beyond. *Ann. Rev. Genet.* 53 (1), 149–170. <https://doi.org/10.1146/annurev-genet-120417-031415>.
- Crosthwaite, S.K., Dunlap, J.C., Loros, J.J., 1997. *Neurospora wc-1* and *wc-2*: Transcription, photoresponses, and the origins of circadian rhythmicity. *Science* (80 . 276 (5313), 763–769.
- Derbyshire, M.C., Michaelson, L., Parker, J., Kelly, S., Thacker, U., Powers, S.J., Bailey, A., Hammond-Kosack, K., Courbot, M., Rudd, J., 2015. Analysis of cytochrome b<sub>5</sub> reductase-mediated metabolism in the phytopathogenic fungus *Zymoseptoria tritici* reveals novel functionalities implicated in virulence. *Fungal Genet. Biol.* 82, 69–84. <https://doi.org/10.1016/j.fgb.2015.05.008>.
- Derbyshire, M.C., Gohari, A.M., Mehrabi, R., Kilaru, S., Steinberg, G., Ali, S., Bailey, A., Hammond-Kosack, K., Kema, G.H.J., Rudd, J.J., 2018. Phosphopantetheinyl transferase (Ppt)-mediated biosynthesis of lysine, but not siderophores or DHN melanin, is required for virulence of *Zymoseptoria tritici* on wheat. *Sci. Rep.* 8, 17069. <https://doi.org/10.1038/s41598-018-35223-8>.
- Desta, I.T., Porter, K.A., Xia, B., Kozakov, D., Vajda, S., 2020. Performance and its limits in rigid body protein-protein docking. *Structure* 28 (9), 1071–1081.e3. <https://doi.org/10.1016/j.str.2020.06.006>.
- Duncan, K.E., Howard, R.J., 2000. Cytological analysis of wheat infection by the leaf blotch pathogen *Mycosphaerella graminicola*. *Mycol. Res.* 104 (9), 1074–1082. <https://doi.org/10.1017/S0953756299002294>.
- Dunlap, J.C., Loros, J.J., 2006. How fungi keep time: circadian system in *Neurospora* and other fungi. *Curr. Opin. Microbiol.* 9 (6), 579–587. <https://doi.org/10.1016/j.mib.2006.10.008>.
- Eyal, Z., Scharen, A.L., Prescott, J.M., van Ginkel, M., 1987. The *Septoria* diseases of wheat: Concepts and methods of disease management, 1st ed. CIMMYT, Mexico.
- Fellows, H., 1962. Effects of light, temperature, and fertilizer on infection of wheat leaves by *Septoria tritici*. *Plant Dis. Reporter* 46, 846–848.
- Fischer, R., Aguirre, J., Herrera-Estrella, A., Corrochano, L.M., Heitman, J., Gow, N.A.R., 2016. The complexity of fungal vision. *Microbiol. Spectr.* 4 (6) <https://doi.org/10.1128/microbiolspec.FUNK-0020-2016>.
- Fones, H., Gurr, S., 2015. The impact of *Septoria tritici* Blotch disease on wheat: An EU perspective. *Fungal Genet. Biol.* 79, 3–7. <https://doi.org/10.1016/j.fgb.2015.04.004>.
- Fones, H.N., Eyles, C.J., Kay, W., Cowper, J., Gurr, S.J., 2017. A role for random, humidity-dependent epiphytic growth prior to invasion of wheat by *Zymoseptoria tritici*. *Fungal Genet. Biol.* 106, 51–60. <https://doi.org/10.1016/j.fgb.2017.07.002>.

- Froehlich, A.C., Liu, Y., Loros, J.J., Dunlap, J.C., 2002. White Collar-1, a circadian blue light photoreceptor, binding to the *frequency* promoter. *Science* 297 (5582), 815–819. <https://doi.org/10.1126/science.1073681>.
- Fuller, K.K., Loros, J.J., Dunlap, J.C., 2015. Fungal photobiology: visible light as a signal for stress, space and time. *Cur. Genet.* 61 (3), 275–288. <https://doi.org/10.1007/s00294-014-0451-0>.
- Glantz, S.T., Carpenter, E.J., Melkonian, M., Gardner, K.H., Boyden, E.S., Wong, G.K.S., Chow, B.Y., 2016. Functional and topological diversity of LOV domain photoreceptors. *Proc. Natl. Acad. Sci. U.S.A.* 113 (11), E1442–E1451. <https://doi.org/10.1073/pnas.1509428113>.
- Goodwin, S.B., Ben M'Barek, S., Dhillon, B., Wittenberg, A.H.J., Crane, C.F., Hane, J.K., Foster, A.J., Van der Lee, T.A.J., Grimwood, J., Aerts, A., Antoniw, J., Bailey, A., Bluhm, B., Bowler, J., Bristow, J., van der Burgt, A., Canto-Canché, B., Churchill, A. C.L., Conde-Ferráez, L., Cools, H.J., Coutinho, P.M., Csukai, M., Dehal, P., De Wit, P., Donzelli, B., van de Geest, H.C., van Ham, R.C.H.J., Hammond-Kosack, K.E., Henrissat, B., Kilian, A., Kobayashi, A.K., Koopmann, E., Kourmpetis, Y., Kuzniar, A., Lindquist, E., Lombard, V., Maliepaard, C., Martins, N., Mehrabi, R., Nap, J.P.H., Ponomarenko, A., Rudd, J.J., Salamov, A., Schmutz, J., Schouten, H.J., Shapiro, H., Stergiopoulos, I., Torriani, S.F.F., Tu, H., de Vries, R.P., Waalwijk, C., Ware, S.B., Wiebenga, A.D., Zwiwers, L.-H., Oliver, R.P., Grigoriev, I.V., Kema, G.H.J., Malik, H.S., 2011. Finished genome of the fungal wheat pathogen *Mycosphaerella graminicola* reveals dispensome structure, chromosome plasticity, and stealth pathogenesis. *PLoS Genet.* 7 (6), e1002070. <https://doi.org/10.1371/journal.pgen.1002070>.
- He, Q., Cheng, P., Yang, Y., Wang, L., Gardner, K.H., Liu, Y., 2002. White collar-1, a DNA binding transcription factor and a light sensor. *Science* 297 (5582), 840–843. <https://doi.org/10.1126/science.1072795>.
- Hevia, M.A., Canessa, P., Müller-Esparza, H., Larrondo, L.F., 2015. A circadian oscillator in the fungus *Botrytis cinerea* regulates virulence when infecting *Arabidopsis thaliana*. *Proc. Natl. Acad. Sci. U. S. A.* 112 (28), 8744–8749. <https://doi.org/10.1073/pnas.1508432112>.
- IBM Corp., 2016. IBM SPSS Statistics for Macintosh, Version 24.0. Armonk, NY: IBM Corp.
- Idnurm, A., Rodríguez-Romero, J., Corrochano, L. M., Sanz, C., Iturriaga, E. A., Eslava, A. P., Eslava, Heitman, J., 2006. The *Phycomyces madA* gene encodes a blue-light photoreceptor for phototropism and other light responses. *Proc. Natl. Acad. Sci. U. S. A.* 103 (12), 4546–4551. <https://doi.org/10.1073/pnas.0600633103>.
- Idnurm, A., Heitman, J., 2005. Light controls growth and development via a conserved pathway in the fungal kingdom. *PLOS Biol.* 3 (4), e95. <https://doi.org/10.1371/journal.pbio.0030095>.
- Idnurm, A., Verma, S., Corrochano, L.M., 2010. A glimpse into the basis of vision in the kingdom *Mycota*. *Fungal Genet. Biol.* 47 (11), 881–892. <https://doi.org/10.1016/j.fgb.2010.04.009>.
- Ingle, R.A., Stoker, C., Stone, W., Adams, N., Smith, R., Grant, M., Carré, I., Roden, L.C., Denby, K.J., 2015. Jasmonate signalling drives time-of-day differences in susceptibility of *Arabidopsis* to the fungal pathogen *Botrytis cinerea*. *Plant J.* 84 (5), 937–948. <https://doi.org/10.1111/tpj.13050>.
- Katebi, A.R., Kloczkowski, A., Jernigan, R.L., 2010. Structural interpretation of protein-protein interaction network. *BMC Struct. Biol.* 10 (Suppl 1), S4. <https://doi.org/10.1186/1472-6807-10-S1-S4>.
- Kalyanamoorthy, S., Minh, B.Q., Wong, T.K.F., von Haeseler, A., Jermini, L.S., 2017. ModelFinder: Fast model selection for accurate phylogenetic estimates. *Nature Methods* 14 (6), 587–589. <https://doi.org/10.1038/nmeth.4285>.
- Kema, G.H.J., Yu, D., Rijkenberg, F.H.J., Shaw, M.W., Baayen, R., 1996. Histology of the pathogenesis of *Mycosphaerella graminicola* in wheat. *Phytopathology* 86 (7), 777–786.
- Kema, G.H.J., van Silfhout, C.H., 1997. Genetic variation for virulence and resistance in the wheat-*Mycosphaerella graminicola* Pathosystem III. Comparative seedling and adult plant experiments. *Phytopathology* 87 (3), 266–272. <https://doi.org/10.1094/PHYTO.1997.87.3.266>.
- Keon, J., Antoniw, J., Carzaniga, R., Deller, S., Ward, J.L., Baker, J.M., Beale, M.H., Hammond-Kosack, K., Rudd, J.J., 2007. Transcriptional adaptation of *Mycosphaerella graminicola* to programmed cell death (PCD) of its susceptible wheat host. *Mol. Plant. Microbe. Interact.* 20 (2), 178–193. <https://doi.org/10.1094/MPMI-20-2-0178>.
- Kim, H., Kim, H.-K., Lee, S., Yun, S.-H., Yu, J.-H., 2015. The White Collar Complex is involved in sexual development of *Fusarium graminearum*. *PLoS One* 10 (3), e0120293. <https://doi.org/10.1371/journal.pone.0120293>.
- Kim, H., Ridenour, J.B., Dunkle, L.D., Bluhm, B.H., He, S., 2011. Regulation of stomatal tropism and infection by light in *Cercospora zeae-maydis*: Evidence for coordinated host / pathogen responses to photoperiod? *PLOS Pathog.* 7 (7), e1002113. <https://doi.org/10.1371/journal.ppat.1002113>.
- Kim, H., Son, H., Lee, Y.-W., 2014. Effects of light on secondary metabolism and fungal development of *Fusarium graminearum*. *J. Appl. Microbiol.* 116 (2), 380–389. <https://doi.org/10.1111/jam.12381>.
- Kim, S., Singh, P., Park, J., Park, S., Friedman, A., Zheng, T., Lee, Y.-H., Lee, K., 2011. Genetic and molecular characterization of a blue light photoreceptor MGWC-1 in *Magnaporthe oryzae*. *Fungal Genet. Biol.* 48 (4), 400–407. <https://doi.org/10.1016/j.fgb.2011.01.004>.
- Koay, B.T., 2010. Investigating polyketide synthase genes of the wheat pathogenic fungus *Mycosphaerella graminicola*. University of Bristol. Thesis 9563. Available via <https://bris.on.worldcat.org/discovery>, last accessed April 2022.
- Kozakov, D., Beglov, D., Bohnuud, T., Mottarella, S.E., Xia, B., Hall, D.R., Vajda, S., 2013. How good is automated protein docking? *Proteins* 81, 2159–2166. <https://doi.org/10.1002/prot.24403>.
- Kozakov, D., Hall, D.R., Xia, B., Porter, K.A., Padjhony, D., Yueh, C., Beglov, D., Vajda, S., 2017. The ClusPro web server for protein-protein docking. *Nat. Protoc.* 12 (2), 255–278. <https://doi.org/10.1038/nprot.2016.169>.
- Larkin, M.A., Blackshields, G., Brown, N.P., Chenna, R., McGettigan, P.A., McWilliam, H., Valentin, F., Wallace, I.M., Wilm, A., Lopez, R., Thompson, J.D., Gibson, T.J., Higgins, D.G., 2007. Clustal W and Clustal X version 2.0. *Bioinformatics* 23 (21), 2947–2948. <https://doi.org/10.1093/bioinformatics/btm3404>.
- Lee, E., Helt, G.A., Reese, J.T., Munoz-Torres, M.C., Childers, C.P., Buels, R.M., Stein, L., Holmes, I.H., Elsie, C.G., Lewis, S.E., 2013. Web Apollo: a web-based genomic annotation editing platform. *Genome Biol.* 14 (8), R93. <https://doi.org/10.1186/gb-2013-14-8-r93>.
- Letunic, I., Bork, P., 2006. Interactive Tree Of Life (iTOL): an online tool for phylogenetic tree display and annotation. *Bioinformatics* 23 (1), 127–128. <https://doi.org/10.1093/bioinformatics/btl529>.
- Letunic, I., Bork, P., 2021. Interactive Tree Of Life (iTOL) v5: an online tool for phylogenetic tree display and annotation. *Nucleic Acids Res* 49 (W1), W293–W296. <https://doi.org/10.1093/nar/gkab301>.
- Linden, H., Macino, G., 1997. White collar 2, a partner in blue-light signal transduction, controlling expression of light-regulated genes in *Neurospora crassa*. *EMBO J.* 16, 98–109. <https://doi.org/10.1093/emboj/16.1.98>.
- Liu, D., Coloe, S., Baird, R., Pedersen, J., 2000a. Rapid mini-preparation of fungal DNA for PCR. *J. Clin. Microbiol.* 38 (1), 471. <https://doi.org/10.1128/JCM.38.1.471-471.2000>.
- Liu, Y.i., Loros, J., Dunlap, J.C., 2000b. Phosphorylation of the *Neurospora clock* protein FREQUENCY determines its degradation rate and strongly influences the period length of the circadian clock. *Proc Natl Acad Sci U. S. A.* 97 (1), 234–239. <https://doi.org/10.1073/pnas.97.1.234>.
- Livak, K.J., Schmittgen, T.D., 2001. Analysis of relative gene expression data using real-time quantitative PCR and the 2<sup>-ΔΔCT</sup> method. *Methods* 25 (4), 402–408. <https://doi.org/10.1006/meth.2001.1262>.
- McCorison, C.B., Goodwin, S.B., 2020. The wheat pathogen *Zymoseptoria tritici* senses and responds to different wavelengths of light. *BMC Genomics* 21, 513. <https://doi.org/10.1186/s12864-020-06899-y>.
- Mohammadi, N., Mehrabi, R., Mirzadi, A.G., Goltapeh, E.M., Safaie, N., Kema, G.H.J., 2017. The ZtVf1 transcription factor regulates development and virulence in the foliar wheat pathogen *Zymoseptoria tritici*. *Fungal Genet. Biol.* 109, 26–35. <https://doi.org/10.1016/j.fgb.2017.10.003>.
- Nguyen, L.-T., Schmidt, H.A., von Haeseler, A., Minh, B.Q., 2015. IQ-TREE: A fast and effective stochastic algorithm for estimating maximum likelihood phylogenies. *Mol Biol Evol* 32 (1), 268–274. <https://doi.org/10.1093/molbev/msu300>.
- Petersen, E.F., Goddard, T.D., Huang, C.C., Couch, G.S., Greenblatt, D.M., Meng, E.C., Ferrin, T.E., 2004. UCSF Chimera - A visualization system for exploratory research and analysis. *J. Comput. Chem.* 25 (13), 1605–1612. <https://doi.org/10.1002/jcc.20084>.
- Poppe, S., Dorsheimer, L., Happel, P., Stukenbrock, E.H., Thomma, B., 2015. Rapidly evolving genes are key players in host specialization and virulence of the fungal wheat pathogen *Zymoseptoria tritici* (*Mycosphaerella graminicola*). *PLOS Pathog.* 11 (7), e1005055. <https://doi.org/10.1371/journal.ppat.1005055>.
- Purschwitz, J., Müller, S., Kastner, C., Schöser, M., Haas, H., Espeso, E.A., Atoui, A., Calvo, A.M., Fischer, R., 2008. Functional and physical interaction of blue- and red-light sensors in *Aspergillus nidulans*. *Curr. Biol.* 18 (4), 255–259. <https://doi.org/10.1016/j.cub.2008.01.061>.
- Quaedvlieg, W., Kema, G. H. J., Groenewald, J. Z., Verkley, G. J. M., Seifbarghi, S., Razavi, M., Mirzadi Gohari, A., Mehrabi, R., Crous, P. W., 2011. *Zymoseptoria* gen. nov.: a new genus to accommodate *Septoria*-like species occurring on graminicolous hosts. *Personia* 26, 57–69. <https://doi.org/10.3767/00315851X571841>.
- RStudio Team (2020). RStudio: Integrated development for R. RStudio, PBC, Boston, MA URL <http://www.rstudio.com/>, last accessed May 2022.
- Rodríguez-Romero, J., Hedtke, M., Kastner, C., Müller, S., Fischer, R., 2010. Fungi, hidden in soil or up in the air: light makes a difference. *Annu. Rev. Microbiol.* 64 (1), 585–610. <https://doi.org/10.1146/annurev.micro.112408.134000>.
- Rudd, J.J., Kanyuka, K., Hassani-Pak, K., Derbyshire, M., Andongabo, A., Devonshire, J., Lysenko, A., Saqi, M., Desai, N.M., Powers, S.J., Hooper, J., Ambroso, L., Bharti, A., Farmer, A., Hammond-Kosack, K.E., Dietrich, R.A., Courbot, M., 2015. Transcriptome and metabolite profiling of the infection cycle of *Zymoseptoria tritici* on wheat reveals a biphasic interaction with plant immunity involving differential pathogen chromosomal contributions and a variation on the hemibiotrophic lifestyle. *Plant Physiol.* 167 (3), 1158–1185. <https://doi.org/10.1104/pp.114.255927>.
- Rueden, C.T., Schindelin, J., Hiner, M.C., DeZonia, B.E., Walter, A.E., Arena, E.T., Eliceiri, K.W., 2017. ImageJ2: ImageJ for the next generation of scientific image data. *BMC Bioinformatics* 18, 529. <https://doi.org/10.1186/s12859-017-1934-z>.
- Sánchez-Arreguín, J.A., Cabrera-Ponce, J.L., León-Ramírez, C.G., Camargo-Escalante, M. O., Ruiz-Herrera, J., 2020. Analysis of the photoreceptors involved in the light-dependent basidiocarp formation in *Ustilago maydis*. *Arch. Microbiol.* 202 (1), 93–103. <https://doi.org/10.1007/s00203-019-01725-w>.
- Schindelin, J., Arganda-Carreras, I., Frise, E., Kaynig, V., Longair, M., Pietzsch, T., Preibisch, S., Rueden, C., Saalfeld, S., Schmid, B., Tinevez, J.-Y., White, D.J., Hartenstein, V., Eliceiri, K., Tomancak, P., Cardona, A., 2012. Fiji: an open-source platform for biological-image analysis. *Nat. Methods* 9 (7), 676–682. <https://doi.org/10.1038/nmeth.2019>.
- Schneider, C.A., Rasband, W.S., Eliceiri, K.W., 2012. NIH Image to ImageJ: 25 years of image analysis. *Nat. Methods* 9 (7), 671–675. <https://doi.org/10.1038/nmeth.2089>.
- Schumacher, J., 2016. DHN melanin biosynthesis in the plant pathogenic fungus *Botrytis cinerea* is based on two developmentally regulated key enzyme (PKS)-encoding genes. *Mol. Microbiol.* 99 (4), 729–748. <https://doi.org/10.1111/mmi.13262>.

- Schumacher, J., 2017. How light affects the life of *Botrytis*. *Fungal Genet. Biol.* 106, 26–41. <https://doi.org/10.1016/j.fgb.2017.06.002>.
- Shaw, M.W., 1991. Interacting effects of interrupted humid periods and light on infection of wheat leaves by *Mycosphaerella graminicola* (*Septoria tritici*). *Plant Pathol.* 40 (4), 595–607. <https://doi.org/10.1111/j.1365-3059.1991.tb02424.x>.
- Shetty, N.P., Mehrabi, R., Lütken, H., Haldrup, A., Kema, G.H.J., Collinge, D.B., Jørgensen, H.J.L., 2007. Role of hydrogen peroxide during the interaction between the hemibiotrophic fungal pathogen *Septoria tritici* and wheat. *New Phytol.* 174 (3), 637–647. <https://doi.org/10.1111/j.1469-8137.2007.02026.x>.
- Talora, C., Franchi, L., Linden, H., Ballario, P., Macino, G., 1999. Role of a white collar-1-white collar-2 complex in blue-light signal transduction. *EMBO J.* 18, 4961–4968. <https://doi.org/10.1093/emboj/18.18.4961>.
- Tiley, A. M. M., 2016. Investigating Asexual Sporulation in *Zymoseptoria tritici*, a Fungal Pathogen of Wheat. University of Bristol. Thesis 11308. ISN:0000 0004 6348 1390. Available at: <https://ethos.bl.uk/OrderDetails.do?uin=uk.bl.ethos.715767>, last accessed April 2022.
- Tiley, A.M.M., Foster, G.D., Bailey, A.M., 2018. Exploring the genetic regulation of asexual sporulation in *Zymoseptoria tritici*. *Front. Microbiol.* 9 (1859), 1–14. <https://doi.org/10.3389/fmicb.2018.01859>.
- Tiley, A.M.M., White, H.J., Foster, G.D., Bailey, A.M., Bailey, A.M., 2019. The *ZvelB* gene is required for vegetative growth and sporulation in the wheat pathogen *Zymoseptoria tritici*. *Front. Microbiol.* 10 (2210), 1–13. <https://doi.org/10.3389/fmicb.2019.02210>.
- Torriani, S.F.F., Melichar, J.P.E., Mills, C., Pain, N., Sierotzki, H., Courbot, M., 2015. *Zymoseptoria tritici*: A major threat to wheat production, integrated approaches to control. *Fungal Genet. Biol.* 79, 8–12. <https://doi.org/10.1016/j.fgb.2015.04.010>.
- Tottman, D.R., 1987. The decimal code for the growth stages of cereals, with illustrations. *Ann. Appl. Biol.* 110 (2), 441–454. <https://doi.org/10.1111/j.1744-7348.1987.tb03275.x>.
- Trifinopoulos, J., Nguyen, L.-T., von Haeseler, A., Minh, B.Q., 2016. W-IQ-TREE: a fast online phylogenetic tool for maximum likelihood analysis. *Nucleic Acids Research* 44 (W1), W232–W235. <https://doi.org/10.1093/nar/gkw256>.
- Vajda, S., Yueh, C., Beglov, D., Bohnuud, T., Mottarella, S.E., Xia, B., Hall, D.R., Kozakov, D., 2017. New additions to the ClusPro server motivated by CAPRI. *Proteins* 85, 435–444. <https://doi.org/10.1002/prot.25219>.
- Wu, C., Yang, F., Smith, K.M., Peterson, M., Dekhang, R., Zhang, Y., Zucker, J., Bredeweg, E.L., Mallappa, C., Zhou, X., Lyubetskaya, A., Townsend, J.P., Galagan, J. E., Freitag, M., Dunlap, J.C., Bell-Pedersen, D., Sachs, M.S., 2014. Genome-wide characterization of light-regulated genes in *Neurospora crassa*. *G3 Genes|Genomes|Genetics* 4 (9), 1731–1745. <https://doi.org/10.1534/g3.114.012617>.
- Yang, J., Zhang, Y., 2015. I-TASSER server: new development for protein structure and function predictions. *Nucleic Acids Res.* 43 (W1), W174–W181. <https://doi.org/10.1093/nar/gkv342>.
- Yu, Z., Fischer, R., 2019. Light sensing and responses in fungi. *Nat. Rev. Microbiol.* 17 (1), 25–36. <https://doi.org/10.1038/s41579-018-0109-x>.
- Zhan, F., Xie, Y., Zhu, W., Sun, D., McDonald, B.A., Zhan, J., 2016. Linear correlation analysis of *Zymoseptoria tritici* aggressiveness with in vitro growth rate. *Phytopathology* 106 (11), 1255–1261. <https://doi.org/10.1094/PHYTO-12-15-0338-R>.
- Zhang, C., Freddolino, P.L., Zhang, Y., 2017. COFACTOR: improved protein function prediction by combining structure, sequence and protein-protein interaction information. *Nucleic Acids Res.* 45 (W1), W291–W299. <https://doi.org/10.1093/nar/gkx366>.
- Zhang, C., Zheng, W., Freddolino, P.L., Zhang, Y., 2018. MetaGO: Predicting gene ontology of non-homologous proteins through low-resolution protein structure prediction and protein-protein network mapping. *J. Mol. Biol.* 430 (15), 2256–2265. <https://doi.org/10.1016/j.jmb.2018.03.004>.